Elsevier Editorial System(tm) for
Construction & Building Materials
Manuscript Draft

Manuscript Number:

Title: Mechanical behaviour of self-compacting concrete made with non-conforming fly ash from coal-fired power plants

Article Type: Research Paper

Keywords: Self-compacting concrete; non-conforming fly ash; siliceous filler; setting reactions; mechanical behaviour; ultrasonic pulse velocity; shrinkage.

Corresponding Author: Dr. José María Fernández Rodríguez, Ph.D.

Corresponding Author's Institution: Universidad de Cordoba

First Author: Alvaro Romero Esquinas

Order of Authors: Alvaro Romero Esquinas; Enrique Fernandez Ledesma; Rocio Otero Izquierdo; José Ramón Jiménez Romero; José María Fernández Rodríguez, Ph.D.

Abstract: Currently, global sustainability depends on achieving integrated productivity in all economic sectors, making it possible to respond to the environmental challenges facing humanity at present. With the dual objective of optimization of natural non-renewable resources and waste recovery, this study has carried out an evaluation of the fly ash of a coal-fired power plant that does not meet the criteria of conformity as a filler in concrete. One may conclude that it is possible to obtain a self-compacting concrete (SCC) by replacing (in volume) a natural siliceous filler (SF) with non-conforming fly ash (NCFA) from coal-fired power plants to obtain a superior mechanical behaviour than the minimum levels stipulated by the Spanish Code on Structural Concrete (EHE-08). The SCC manufactured with NCFA partially presented good performance in terms of self-compactability, mechanical behaviour, and shrinkage. To achieve these results, a comparative study of three mixes of SCC was carried out. In the first (SCC-1), a commercial SF (SCC reference) was used; in the second a mix, 1: 1 in volume, SF and NCFA (SCC-12) was used; and in the third, only NCFA was used (SCC-2). The mechanisms for setting the mixes have been identified. Pozzolanic and mild carbonation reactions were present in the SCC-1 mix. In SCC-12, both pozzolanic and carbonation reactions were observed. In the SCC-2 mix, only carbonation processes were observed. The mechanical behaviour of the SCC-1 and SCC-12 mixes is better than that of SCC-2. The incorporation of NCFA as a filler in SCCs resulted in better shrinkage performance at an early age, and therefore, less cracking.

**Highlights**

- A comparative study of three types of SCC was carried out
- The mixes comply with the self-compacting requirements stipulated by the EHE-08
- The aging mechanisms of the SCC mixes (SCC-1, SCC-12, and SCC-RF) were different
- Pozzolanic reactions occurred during the curing of SCC-1
- Shrinkage in the NCFA mix was lower because of the larger particle size
- Non-conforming fly ash from coal-fired power plants is adequate to produce SCC

**Graphical Abstract**

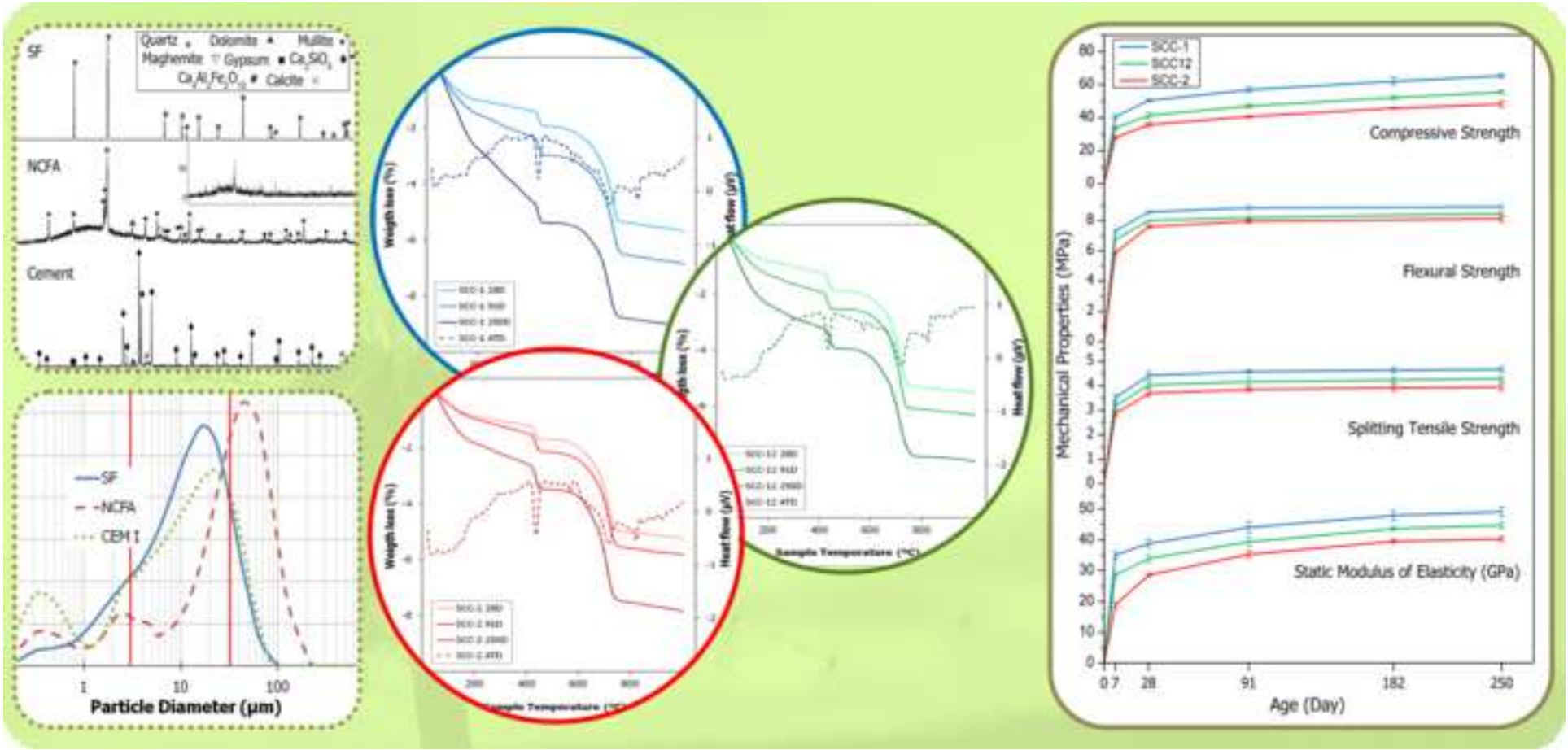

# Mechanical behaviour of self-compacting concrete made with non-conforming fly ash from coal-fired power plants

**A. R. Esquinas [a], E. F. Ledesma [b], R. Otero [c], J.R. Jiménez [d,*] and J.M. Fernández [a,e,*]**

[a]*Departamento de Química Inorgánica e Ingeniería Química, Escuela Politécnica Superior de Belmez, Universidad de Córdoba, Avenida de la Universidad s/n. E-14240 Belmez (Córdoba), España.*

[b]*Area de Mecánica de los Medios Continuos y Teoría de Estructuras, Universidad de Córdoba, Edificio Leonardo Da Vinci, Campus de Rabanales, E-14071 Córdoba, España*

[c]*Instituto Universitario de Investigación en Química Fina y Nanoquímica IUIQFN, Facultad de Ciencias, Universidad de Córdoba, Campus de Rabanales, Edificio Marie Curie, E-14071 Córdoba, España*

[d] *Área de Ingeniería de la Construcción, Universidad de Córdoba, Edificio Leonardo Da Vinci, Campus de Rabanales, E-14071 Córdoba, España*

[e] *Departamento de Química Inorgánica e Ingeniería Química, Instituto Universitario de Investigación en Química Fina y Nanoquímica IUIQFN, Facultad de Ciencias, Universidad de Córdoba, Campus de Rabanales, Edificio Marie Curie, E-14071 Córdoba, España.*

* Corresponding authors. Both authors contributed equally to the manuscript.

Address:

- Departamento de Química Inorgánica e Ingeniería Química, Escuela Politécnica Superior de Belmez, Universidad de Córdoba, Avenida de la Universidad s/n. E-14240

Belmez (Córdoba), España. Tel.: +34 618808043; fax: +34 957580644 (J.M. Fernández).

- Área de Ingeniería de la Construcción, Universidad de Córdoba, Edificio Leonardo Da Vinci, Campus de Rabanales, E-14071 Córdoba, España. Tel.: +34 667524702; fax: +34 957218550. (JR Jiménez)

*E-mail address:* um1feroj@uco.es (JM Fernandez); jrjimenez@uco.es (JR Jiménez)

**Abstract**

Currently, global sustainability depends on achieving integrated productivity in all economic sectors, making it possible to respond to the environmental challenges facing humanity at present. With the dual objective of optimization of natural non-renewable resources and waste recovery, this study has carried out an evaluation of the fly ash of a coal-fired power plant that does not meet the criteria of conformity as a filler in concrete. One may conclude that it is possible to obtain a self-compacting concrete (SCC) by replacing (in volume) a natural siliceous filler (SF) with non-conforming fly ash (NCFA) from coal-fired power plants to obtain a superior mechanical behaviour than the minimum levels stipulated by the Spanish Code on Structural Concrete (EHE-08). The SCC manufactured with NCFA partially presented good performance in terms of self-compactability, mechanical behaviour, and shrinkage. To achieve these results, a comparative study of three mixes of SCC was carried out. In the first (SCC-1), a commercial SF (SCC reference) was used; in the second a mix, 1: 1 in volume, SF and NCFA (SCC-12) was used; and in the third, only NCFA was used (SCC-2). The mechanisms for setting the mixes have been identified. Pozzolanic and mild carbonation reactions were present in the SCC-1 mix. In SCC-12, both pozzolanic and carbonation

reactions were observed. In the SCC-2 mix, only carbonation processes were observed. The mechanical behaviour of the SCC-1 and SCC-12 mixes is better than that of SCC-2. The incorporation of NCFA as a filler in SCCs resulted in better shrinkage performance at an early age, and therefore, less cracking.

**Key words:** Self-compacting concrete; non-conforming fly ash; siliceous filler; setting reactions; mechanical behaviour; ultrasonic pulse velocity; shrinkage.

**Highlights:**

- A comparative study of three types of SCC was carried out
- The mixes comply with the self-compacting requirements stipulated by the EHE-08
- The aging mechanisms of the SCC mixes (SCC-1, SCC-12, and SCC-RF) were different
- Pozzolanic reactions occurred during the curing of SCC-1
- Shrinkage in the NCFA mix was lower because of the larger particle size
- Non-conforming fly ash from coal-fired power plants is adequate to produce SCC

## 1. Introduction

Innovation and research are the key to the implementation of a circular economy in the construction sector, which is fundamental for the sustainability of the current world. Along these lines, the European Union (EU) has indicated the actions and compromises in all economic sectors to achieve the optimization of natural resources, as well as the minimization and valorisation of waste, managing to respond to environmental

challenges [1]. In the construction sector, the concrete industry stands out, since concrete is the most widely used construction material [2, 3].

Self-compacting concrete (SCC) was developed in Japan by Professor Okamura in the mid-1980s [4]. The main feature of this type of concrete is the ability to flow and completely fill the entire volume of the formwork by the action of its own weight [5]. This allows for the execution of complex and densely reinforced structures with more complex designs, owing to the great fluidity, cohesion, homogeneity, resistance to segregation, and extraordinary surface finishes that SCC possesses [6, 7]. SCC needs to incorporate a high content of fines (cement, filler, and/or fine aggregates) and chemical additives in its dosage. This particularity means that the SCC can be considered as not very environmentally friendly. Nowadays, a solution would be to use materials of a residual nature as a substitute for the conventional raw materials used in the manufacture of the SCC. This would allow the minimization and valorization of this waste, as well as the optimization of the natural resources used.

Sharma and Khan [8] used copper slag with different percentages of fine aggregate substitution. The results of their research showed the improvement of the self-compactability properties with the increase in the percentage of substitution. The authors concluded that using 60% copper slag resulted in the mechanical behaviour and durability of the SCC being better than or comparable to that of the reference SCC. Subasi et al. [9] used waste ceramic powder as a filler, and this had a positive effect on the viscosity of the mixes, although the strength suffered a slight reduction. Gesoglu et al. [10] incorporated plastic waste powder in the SCC in different percentages of cement replacement. These authors obtained a 24.6% reduction in compression strength in

mixes that used 25% of this by-product compared to the reference, although the concretes became less brittle. Esquinas et al. [11, 12] developed SCC, incorporating a dolomitic waste powder from the drying of the aggregates of the hot bituminous mixes as a substitute for the commercial filler of siliceous nature, and they reported good mechanical behaviour and durability.

By-products generated during combustion in different industrial processes have been evaluated for application as raw materials in the SCC by different researchers. Gill and Siddique [13] used rice-husk ash as a substitute for fine aggregates. The experimental results indicated that the mixes with this waste met the requirements of self-compactability and mechanical behaviour. Ranjbar et al. [14] observed the great potential of palm oil fuel ash as a substitute for cement in SCC due to the acceptable results obtained regarding the parameters of selfcompactability, mechanical behaviour, and durability. The application of the ashes in SCC, resulting from the combustion of agricultural residues in biomass-fired power plants as a filler was investigated by Cuenca et al. [15]. These researchers showed that the use of biomass ash was favourable to the mechanical behaviour of the SCC.

The most studied by-product from combustion processes has been the fly ash (FA) from coal-fired power plants that meets the criteria of compliance specified by the standards EN 450-1, EN 450-2, EN 14227-4, and ASTM C 618 [16, 17] (conforming fly ash), and is characterized by its pozzolanic nature [18-21].

When the FA does not comply with the required fineness, i.e., when the mass retained on the 0.045-mm sieve is greater than 40%, the FA is considered as non-conforming fly

ash (NCFA). This by-product represents between 30% and 40% of the total production of FA and it is destined to landfill, significantly impacting the environment [22]. In addition, we must consider the fact that the global production of FA is estimated at 750 million tons, of which 100 million tons are generated in Europe [23, 24].

This is a very serious environmental problem since coal will continue to be the most-used fuel for decades, according to the estimates of the International Energy Agency [25]. The FA resulting from the combustion of coal, in accordance with Directive 2008/98/EC of the European Union (European Waste Framework Directive), is considered as waste and must be recovered to achieve the end-of-waste (EoW) status before it may be used again [26].

In the present work, the use of NCFA has been evaluated as a filler in SCC. A comparative study of three SCCs mixes was carried out; in the first mix, a commercial siliceous filler (SF) was used as a reference; in the second a mix, 1:1 in volume, of SF and NCFA was used; and in the third, only NCFA was used. The amount of filler used in volume is similar in all cases. To determine the behaviour of the three SCCs, a fresh-state study was carried out first, and self-compatibility properties were studied, such as fluidity, blocking resistance, and resistance to segregation. Subsequently, a deep analysis of hardened SCCs was carried out, including their mechanical behaviour in the long term and their correlation with the different chemical reactions that occur during setting time. Finally, a short-term shrinkage study is also included to allow a response to the mechanical requirements demanded for the use of this waste.

## 2. Experimental methodology

148

149 **2.1. Materials**

150

151 The aggregates used were gravel 4/16 (G), coarse sand 0/4 (S1), and fine sand 0/2 (S2),
152 which come from the crushing plant owned by Charamuzca Movimiento de Tierras,
153 Áridos, and Hormigones SL (Córdoba, Spain). Their grading curves are shown in
154 Figure 1. The physical–chemical characterization is shown in Table 1. The aggregates
155 are suitable for the manufacture of concrete, according to the Spanish Instruction for
156 Structural Concrete (EHE-08) [27]. In the X-ray diffractogram (Figure 2), it was
157 observed that the main phase was quartz (33-1161) [28]; in addition, the presence of
158 calcite (05-0586) [28], orthoclase (31-0966) [28], albite (41-1480) [28], and clinochlore
159 (16-0362) [28] was observed.

160

161 The commercial filler is of siliceous nature and comes from the Mines Carmina of the
162 company Lorda and Roig S.A. (Gerona, Spain). The NCFA comes from the Puente
163 Nuevo coal-fired power station (Córdoba, Spain) of Viesgo electric company.
164 According to UNE-EN 933-1 [16], the particle size distribution of these materials was
165 as follows: 100% of both fillers pass through the 2-mm sieve; 100% and 92.4% of SF
166 and NCFA, respectively, pass through the 0.25-mm sieve; 100% and 59.6% of SF and
167 NCFA, respectively, pass through the 0.125-mm sieve; and 74.33% and 27.5% of SF
168 and NCFA, respectively, pass through the 0.063-mm sieve. Consequently, the SF is in
169 accordance with the requirements set by the EHE-08, and the NCFA presents a size
170 distribution somewhat greater than the one specified by the instruction, (70% goes
171 through the 0.063-mm sieve, 85% goes through the 0.125-mm sieve, and 100% goes
172 through the 2-mm sieve [16]). In addition, an analysis of the grain size distribution was

carried out by laser diffraction, using ethanol as the dispersant (Figure 3). The NCFA has a wider distribution than the SF (0.1–240 μm vs 0.1–100 μm). The highest percentage of particles is around 20 μm for the SF and around 45 μm for the NCFA. The SF has the highest percentage of particles between 3 and 32 μm (71.28%). In the NCFA, the percentage of particles found between 3–32 μm is 39.64% (Table 2). These results are significant, since above 32 μm (11.59% for the SF vs 45.01% for the NCFA), the particles are too large to fully hydrate, and below 3 μm (17.13% for the SF vs 15.35% for the NCFA), make only a small contribution to the mechanical strength and simultaneously demand more water [29-31]. Moreover, this large number of particles whose size exceeds 45 μm prevents their use as a mineral addition for concrete production, in accordance with UNE-EN 450-1:2003 [16], and hence the name "non-conforming fly ash".

The X-ray diffraction (XRD) patterns (Figure 4) revealed that quartz is the only phase of SF present (33-1161) [28], which has a high crystallinity. In the NCFA, besides quartz (33-1161) [28], the presence of mullite (15-0776) [28], dolomite (36-0426) [28], and maghemite ($\gamma$-$Fe_2O_3$) (25-1402) [28] were observed, along with a non-negligible percentage of amorphous phase. The thermogravimetric analysis of the fillers (Figure 5) shows the purity of the SF filler, since no thermal effect is observed. In the case of NCFA, an endothermic peak is observed, which corresponds to a small weight loss (1.2%) between 500 and 700 °C, indicating the decomposition of dolomite.

The Brunauer–Emmett–Teller (BET) surface of both samples (SF and NCFA) was very small, at 2.90 $m^2/g$ and 1.80 $m^2/g$, respectively (Table 2). The pore size distribution, obtained from the adsorption–desorption isotherms of nitrogen, is shown Figure 6. Both

fillers show a range of pore diameter between 2.5–37 nm, according to the DFT method. The distribution of pore volume is comparable in both materials, although for the NCFA, the range in which the highest quantity of pore volume is centred was slightly lower than SF (2.5–6 nm vs. 2.5–9 nm). Both samples have mesopores of small size, below 10 nm, and the maximum of the pore volume distribution is around 3.2 nm, which is very close to the micropore area (< 2 nm).

The cement used was type CEM I 42,5 R/SR (UNE 80303-1 and UNE-EN 197-1) [16]. Figure 3 shows the particle size distribution, which, as in the SF, has the highest percentage of particles between 3 and 32 μm (59.96%) (Table 2), and this is important for the hydration process, as mentioned previously. The chemical composition, expressed in the form of oxides, determined by energy-dispersive X-ray analysis (EDX), is shown in Table 2. The majority oxide was calcium oxide (CaO), highlighting that the content of aluminium oxide ($Al_2O_3$) was very low. The X-ray diffractogram (Figure 4) showed that the majority mineral phase was tricalcium silicate, $Ca_3SiO_5$ (42-0551) [28], and a small proportion of gypsum, $CaSO_4 \cdot H_2O$ (33-0311) [28] and calcium ferroaluminate, $Ca_4Al_2Fe_2O_{10}$, (11-0124) [28], were detected.

An additive, superplasticizer/water reducer with high performance, was used, specific for SCC (sp), Glenium 303 SCC BASF Chemical Company, and the objective was to manufacture SCC with a low water/cement ratio (W/C).

### 2.2. Concrete mixes and composition tests

Three mixes (SCC-1, SCC-2, and SCC-12) were designed according the composition of Esquinas et al. [12], with a quantity of gravel of approximately 800 kg/m$^3$, and a minimum amount of cement of 400 kg/m$^3$. For all mixes, the specific design requirements were marked: exposure class IIIc, characteristic strength of 40 MPa, cement content 400 kg/m$^3$, maximum ratio W/C = 0.44, and the same amounts of additive (1.8% cement + filler) and cement. According to the EHE-08, it was classified as HA-40/AC/16/IIIc. The adjustment of the dosage was made in volume (1025 L) [32].

To study the effect of the NCFA, as a filler, on the properties of SCC, three types of mixes were designed: SCC-1, SCC-2, and SCC-12, with commercial filler, with NCFA, and with a 1:1 mix (by volume) of both materials. For all mixes, we proceeded to the study the self-compactability according to the requirements of the EHE-08 [27].

The SCC-1 mix, whose composition in dry weight and volume is shown in Table 3, was considered as reference concrete. The three dosages met the recommendations of the European Federation of National Associations Representing Producers and Applicators of Special Building Products for Concrete (EFNARC) (Table 3) [6, 7].

To realize SCCs with NCFA (SCC-2 and SCC-12), maintaining the same filler volume as the reference dosage (SCC-1) and with a similar granular skeleton, small adjustments of the total content of aggregates and water were made, as well as of the relation 0/2 sand with respect to the filler (Table 3). It can be observed that the percentage of the different materials in the mixes were similar.

### 2.3. Test methods

247

248 The raw materials, as well as the hardened SCC, were characterized using different
249 techniques. Particle sizes were measured in a Mastersizer S analyser (Malvern
250 Instruments), using ethanol as the dispersant. The samples were analysed through XRD
251 patterns by using a Bruker D8 Discover A25 instrument with CuKα radiation. SF and
252 cement diffraction patterns were obtained by scanning the goniometer from 10° to 70°
253 (2θ), at a rate of 0.05° $min^{-1}$. For NCFA, the rate was 0.006° $min^{-1}$ (additionally, for
254 comparison, the spot inside a XRD pattern for NCFA, at a rate of 0.05° $min^{-1}$, was
255 made). The thermogravimetric analysis was carried out in a Setaram Setsys Evolution
256 16/18 apparatus, at a heating rate of 5 °C/min. Specimens (150 × 150 × 150 mm) were
257 kept in an oven at 100 °C. Then, a little portion (a cube of 10 × 10 × 10 mm) was taken
258 from the centre of the specimen for performing the thermic analysis (DTA-TGA). The
259 tangent method was used to identify the temperature range of chemical species
260 decomposition [33]. $N_2$ isotherms were determined on an Autosorb iQ (Quantachrome),
261 and samples were degassed at 100 °C under vacuum for 2 h prior to this. The surface
262 was calculated by applying the BET method in the range of relative equilibrium
263 pressure $0.05 \leq P/Po \leq 0.20$ [34].
264
265 Microstructural characterization of the materials was carried out using an electron
266 microprobe technique implemented on a JEOL JSM-7800F scanning electron
267 microscope, using an acceleration voltage of 15 kV and a working distance of 10 mm.
268 The X-ray detector was an X-MaxN150 from Oxford Instruments.
269
270 The self-compactability of mixes were studied according to the requirements of EHE-08
271 (Table 4). The compressive strength (UNE-EN 12390-3) [16] and the splitting tensile

strength (UNE-EN 12390-6) [16] were measured in cylindrical specimens of 300 mm × 150 mm, and flexural strength (UNE-EN 12390-5) [16] was measured in prismatic specimens of 100 × 100 × 40 mm, for the ages 7, 28, 91, 182, and 250 days, cured in water, in accordance with UNE 12390-2 [16]. The secant modulus of elasticity in compression (UNE-EN 12390-13) [16] was studied at ages of 7, 28, 91, 182, and 250 days in cylindrical specimens of 300 mm × 150 mm. For this group of tests, a IBERTEST model MEH-3000 press with a maximum capacity of 3,000 kN was used.

The ultrasonic pulse velocity (UPV) (UNE-EN 12504-4) [16] was evaluated at the ages of 7, 28, 91, 182, and 250 days for concrete, using an ultrasonic flow meter from Matest, model C369N. Related to this parameter, the density values (fresh, wet, and dry) (UNE-EN 12390-7 and UNE-EN12350-6) [16] in 150 × 150 × 150 mm specimens cured in water were determined. A total shrinkage study (ASTMC157 / C157M-08e1) [17] during the time of the retraction test, at a young age (up to 91 days), was performed on specimens with dimensions of 100 × 100 × 500 mm. For this test, the specimens were kept in a curing chamber under constant environmental conditions, at a temperature of 20 °C and a relative humidity of 50%. All tests were triplicated, in specimens made from the same SCC mix, showing average values and standard deviations.

## 3. Results and discussion

### 3.1. Properties of SSC in fresh state

#### 3.1.1. Self-compactability

297

298 Table 5 shows the self-compactability parameters of the three mixes, which agree with
299 the parameters specified by the EHE-08 [27] (Table 4). For the parameter $T_{50}$, the
300 values 2.34 s, 2.69 s, and 4.35 s were obtained; for the $d_f$ parameter, 725.13 mm, 676.75
301 mm, and 699 mm were achieved; for the parameter $d_f$ - $d_{Jf}$, the results were 38, 24, and
302 25; for $C_{bL}$, it reached 0.92, 0.84, and 0.82; and finally, for Tv, the results were 7.13 s,
303 11.10 s, and 10.07 s, corresponding to the mixes SCC-1, SCC-2, and SCC-12,
304 respectively.

305

306 Figure 7 shows the workability of the mixes based on $d_f$ and Tv [35]. (Four repetitions
307 were made for each mix, and the averages were represented by a solid square, a solid
308 triangle, and a solid circle, respectively). Note that all mixes are within the area in
309 which the SCC would have good self-compactability. For the specific case of SCC-1
310 (mix with SF), the mix is located in the region known as "Marginal SCC area," an area
311 in which there could be a slight segregation, according to the author, although this
312 aspect was not observed in none of the mixes of the present work, since a good
313 distribution of the coarse aggregate was observed, and there are no signs of segregation
314 and bleeding, which is in accordance with the proximity to the area called "Proper SCC
315 area." SCC-2 (mix with NCFA) and SCC-12 (mix 1:1 of SF and NCFA) remain inside
316 the "Proper SCC area" box, that is, they are considered as appropriate and acceptable
317 SCCs. Additionally, the reproducibility of the mixes in all the repetitions could be
318 observed.

319

320 The differentiated behaviour of the mixes SCC-1 and SCC-2 in terms of the workability
321 may be mainly due to the greater particle size presented by NCFA (Figure 3), which

results in a lower content of fines and volume of the paste (Table 3), causing a greater difficulty to flow, compared to the results obtained in the reference mix (SCC-1). This behaviour is in accordance with the greater amount of water (182.75 $L/m^3$ vs 176.93 $L/m^3$) necessary to achieve the self-compactability of the SCC-2 mix. A reduction in $d_f$ equal to -7% and an increase in Tv equal to 56% was observed. These percentages are reduced in the SCC-12 mix, around -4% for $d_f$ and 41% for Tv, compared to the SCC-2 mix; the SCC-12 mix presents a greater fluidity when incorporating 50% in volume of the commercial filler. This may be due to the improvement of the particle size distribution of the filler when a 1:1 mix of both materials is incorporated, which may result in a better packing factor of the finer particles, and therefore, an improvement in self-compactability properties. This result is in agreement with the fine material and paste content, which is intermediate compared to the other mixes (SCC-1 and SCC-2).

These results show that it is possible to obtain SCC within the parameters specified by the EHE-08, using the NCFA residue as the filler, and starting from a dosage in which the natural SF is replaced by NCFA, from 50% to 100% in volume.

These results are in agreement with those obtained by Esquinas et al. [11, 12], who observed a similar behaviour when the SF was replaced by a dolomitic residual powder. This residue had a larger particle size than the SF, of the same order as that observed in the NCFA sample. The self-compactability, as in the present work, is closer to the limits given by the EHE-08, and hence the SCC can be considered as adequate and acceptable, with regard to workability. Silva and de Brito [36] obtained good self-compactability results in dosages that used as a filler a mix of limestone filler and fly ash, in volumetric proportions of 2:1 and 1:2. On the other hand, when in the mixes, conforming fly ash is

introduced for use in concrete, the behaviour differs from that observed in this work, since there is an improvement in self-compactability (in terms of filling and passing ability) compared to the reference SCC, as can be seen in the work carried out by Suaiam et al. [20]; this could be due mainly to a fine particle size distribution (< 45 μm) that characterizes this material.

#### 3.1.2. Density of SCC in fresh state

The fresh density values recorded for SCC-1, SCC-12, and SCC-2 were 2.441 kg/dm$^3$, 2.421 kg/dm$^3$, and 2.397 kg/dm$^3$, respectively. The higher density of SCC-1 relative to the other mixes may be due to the finer and more continuous particle size distribution of the SF compared to the NCFA (Figure 3). On the other hand, the higher content of fines presents in the SCC-1 mix (Table 3) would be in accordance with the results obtained, since it would yield a higher packing density. These results are in agreement with the densities obtained by other researchers [11, 12, 37].

### 3.2. Properties of SSC in hardened state

#### 3.2.1. Physical–chemical characterization of hardened SCC

By means of the thermal analysis, TGA-DTA (Figure 8) (only one heat flow curve has been included because the information, for the propose of this paper, was the same), the different processes during the curing of the SCCs were identified. Three zones can be differentiated: in the first zone, from room temperature to 400 ºC, corresponding to the loss of free water physically adsorbed (until 100 ºC, negligible in the samples studied in

this work, since they have been kept in an oven at 100 ºC until constant weight), the loss of interlaminar water, the loss of structural water due to the dehydration processes of hydrated silicates and calcium aluminates, and the water present in the pores. The second zone, between 400 ºC and 550 ºC, corresponds to the dehydroxylation of the portlandite. The third zone, between 550 ºC and 750 ºC, is due to the decomposition of carbonates, initial or formed in the setting process. Finally, from 750 °C, there is a loss corresponding to the elimination of OH residues.

SCC-1 presented a greater degree of hydration with the curing time. The degree of hydration at 250 days was 4.54%, 3.16%, and 2.55% for SCC-1, SCC-12, and SCC-2, respectively (Table 6). In the column "$H_2O_{Total}$" of Table 6, it is observed that there is an increase in the water content with curing time in all the mixes. A greater water content is observed at 250 days in the samples of SSC-1 and SCC-12 compared to the SCC-2 mix. This can be attributed to the pozzolanic reaction of the SF with $Ca(OH)_2$ to form CSH, which is in accordance with the lower increase in the total $Ca(OH)_2$ content that occurs in the SCC-1 mix, followed by SCC-12, compared to SCC-2 for the same curing time.

The amount of $Ca(OH)_2$, which corresponds to the hydration process of the calcium silicates, was determined by the weight loss recorded between 400 ºC and 550 ºC. This amount increases with the time of setting in all the SCCs, since the amount of cement present in the mixes is the same.

The carbonate content was higher in the SCC-2 mix, as observed in the weight loss between 550 °C and 750 °C (Figure 8 and Table 6), followed by the SCC-12 and SCC-1

mixes. The first column of "$CaCO_3$" in Table 6 represents the content of $CaCO_3$ that has been formed by carbonation of $Ca(OH)_2$, and has been calculated from the weight loss between 550 ºC and 750 ºC, from which is subtracted the content of $CaCO_3$ initially present in the aggregates of the mixes (second column of "$CaCO_3^{(a)}$" of Table 6), estimated at 6.6% (159 kg/m$^3$) of the mix. The carbonation of the mixes grows slightly with the setting time, although for the SCC-12 and SCC-2 samples at 250 days, this increase is more important (Table 6). Therefore, in the total content of portlandite, the amounts of carbonate formed from $Ca(OH)_2$ should be taken into account, and are shown in the "$Ca(OH)_{2\ Total}$" column of Table 6.

A correlation was established between the values of the columns "$Ca(OH)_{2\ Total}$" and "$H_2O_{Total}$" of Table 6 (without taking into account the values for 250 days of curing of the mixes SCC-1 and SCC-12, as previously mentioned, regarding the presence of pozzolanity). We used the equation ($y = 0.5236\ x - 8.0445$) to obtain the theoretical portlandite ($Ca(OH)_2$) quantity for the SCC-1 and SCC-12 mixes after 250 days, without taking into account the pozzolanic reaction. The values obtained were 227.5 kg/m$^3$ and 161.7 kg/m$^3$, respectively, and are superior to the experimental values $Ca(OH)_{2\ Total}$ (Table 6). For the SCC-2 mix, the theoretical total amount of $Ca(OH)_2$ obtained according to the aforementioned correlation was 132.8 kg/m$^3$, which is very similar to the experimental quantity $Ca(OH)_{2Total}$.

The XRD patterns are shown in Figures 9 and 10. In Figure 9, the evolution of the phases presents in the mixes SCC-1 and SCC-2 during short-term curing (up to 91 days) was analysed. Figure 10 shows the phases present in the three mixes (SCC-1, SCC-12,

and SCC-2) during long-term curing (250 days). The main phases observed in a short curing age were quartz (33-1161), portlandite (04-0733), and calcite (05-0586), and to a lesser extent ettringite (41-1451), albite (09-0466), orthoclase (31-0966), $Ca_2SiO_4$ (31-0297), and illite (02-0056) [28]. At high curing times (250 days) (Figure 10), there is a decrease in the peaks corresponding to portlandite with respect to the peaks corresponding to quartz for the SCC-1 sample due to the pozzolanic reaction that occurs between the portlandite and the SF. On the other hand, in the SCC-12 and SCC-2 mixes, an increase of the content of portlandite with respect to the content of quartz is observed.

This is in accordance with the greater weight loss suffered by SCC-1 between 0 and 400 ºC (dehydration zone), and in SCC-2, the greatest weight loss occurs in the decarbonation zone (550-750 ºC). It can be concluded that the setting mechanism of both concretes (SCC-1 and SCC-2) is different, depending on the nature of the filler added. In the case of the SCC-12 mix, the behaviour is intermediate. In short, pozzolanic and slight carbonation reactions occur in the SCC-1 mix. In SCC-12, both pozzolanic and carbonation reactions are observed, whereas in the SCC-2 mix, only carbonation processes are observed.

In summary, it can be concluded that in the SCC-1 and SCC-12 mixes, there would be a pozzolanic reaction, which is more intense in the SCC-1 mix, where only SF was used as the filler. On the other hand, when only NCFA was used as the filler, this reaction was not observed, and hence, the total content of $Ca(OH)_2$ was higher. This is in accordance with the greater percentage of particles of size greater than 32 μm presented by the NCFA, as mentioned in the section Materials and Methods.

### 3.2.2. Density of SCC

The three mixes have similar wet density values (measured at 28 days), although the mixes that incorporate NCFA have slightly lower values: 2.418 kg/dm$^3$ (SCC-12) and 2.398 kg/dm$^3$ (SCC-2), compared to 2.438 kg/dm$^3$ of the reference mix (SCC-1). This is in accordance with the dosages of the three mixes (Table 3), in which the presence of NCFA causes a decrease in the wet density of the mix with this waste.

The dry density values (after the drying process at 105 ºC to constant mass) follow the same pattern as that observed for wet density: 2.329 kg/dm$^3$, 2.323 kg/dm$^3$, and 2.284 kg/dm$^3$ for SCC-1, SCC-12, and SCC-2 mixes, respectively. If a comparative analysis of both densities is carried out, it can be concluded that the loss of free water in the drying process was approximately 4.5% in the three mixes. This behaviour is influenced by the effective water content present in the mixes: 17.28%, 17.52%, and 17.85% for SCC-1, SCC-12, and SCC-2 mixes, respectively, and will in turn have an influence on the mechanical behaviour of the SCCs.

These results are in agreement with those obtained by other authors such as Esquinas et al. [12], who observed a decrease in density when replacing a commercial SF with a fine granulometry residue of dolomitic nature and of larger particle size in the mix. Barbhiya [38] observed a lower density in mixes that incorporated FA compared to mixes using a commercial dolomitic filler, with a microfiller effect caused by the fine grain of dolomite powder.

Additionally, the higher density of the SCC-1 mix is favourably influenced by the pozzolanic reactions that fill the gaps of the granular skeleton, compared to the SCC-2 mix.

### 3.2.3. Compressive strength

The compressive strength of SCC-2, which uses NCFA as the filler, is lower than that of SCC-1 (used as a reference). The partial use of this by-product together with the commercial SF (SCC-12 mix) caused an increase in the compressive strength compared to the mix with 100% of the by-product (SCC-2) (Figure 11).

The compressive strength values for the SCC-1 mix at 7, 28, 91, 182, and 250 days were 40.67, 50.30, 56.87, 61.99, and 65.32 MPa, respectively. For the SCC-12 mix, the results obtained were 33.83, 41.27, 47.01, 52.05, and 55.64 MPa, respectively. For the SCC-2 mix, the values were 28.02, 35.67, 40.66, 45.69, and 48.77 MPa. At early ages of curing (7 days), there is a greater difference in the compressive strength compared to the SCC-1 mix; 16.8% and 31% for SCC-12 and SCC-2, respectively. The delay in hydration observed in these mixes may be due to the greater particle size distribution of the NCFA, (45% of the particles are greater than 32 μm versus 12% in the SF) (Figure 3), which would make the complete hydration of the particles, and consequently, the mechanical development, difficult.

From the age of curing of 28 days, in the SCC-2 mix, there is a slower compressive strength increase than in the SCC-1 mix, since the slope of the trend lines is 5.7% and 6.8%, respectively. The SCC-12 mix presents an intermediate evolution to these values

(6.5%). The only factor that differentiates these dosages is the type of filler used, and therefore, this is responsible for the difference in mechanical behaviour. In short, the greater compressive strength of SCC-1 may be due to the particle size distribution of the SF used (71% of the particles have sizes between 3 and 32 μm, Figure 3) [39-41]. This evolution is in agreement with the experimental data obtained with the thermogravimetric and DRX analyses of the mixes (Table 6 and Figures 9 and 10), which show a decrease in the content of portlandite in the SCC-1 and SCC-12 mixes, compared to the SCC-2 mix (without SF), as already mentioned in the section on characterization of the hardened mixes.

This behaviour is in agreement with the results obtained by Esquinas et al. [12], who observed a decrease in the compressive strength of the SCC that incorporated a dolomitic waste compared to the SCC with a commercial silicon filler. These by-products caused a delay in the hydration of the SCC due to a greater particle size distribution, as is the case of the NCFA. On the other hand, Dadsetan and Bai [19] carried out a study on the mechanical behaviour of SCC with different types of fillers, observing that the mixes with fly ash had a lower compressive strength compared to mixes with metakaolin and ground granulated blast-furnace slag, mainly due to the high pozzolanic activity of these two additions, similar to the evolution observed in the present work. Finally, Silva and Brito [42] observed an increase in the compressive strength of SCC with conforming FA regarding an addition of a limestone filler, owing to a thicker particle size distribution and absence of pozzolanity.

The results obtained show that it is possible to use NCFA from coal-fired power plants as the filler and achieve compressive strengths above the minimum levels stipulated by

522 the Spanish Structural Concrete Code [27] for a HAC-30. If a mix (1:1) of NCFA +
523 commercial SF is added to SCC, strength higher than 40 MPa can be obtained after 28
524 days, with a 15% reduction in compressive strength compared to the reference mix.
525
526 **3.2.4. Splitting tensile strength**
527
528 The results of splitting tensile strength of the different mixes at 7, 28, 91, 182, and 250
529 days are shown in Figure 11. For SCC-1, the splitting tensile strength values obtained
530 were 3.51, 4.42, 4.57, 4.63, and 4.67 MPa, respectively. For SCC-12, they were 3.16,
531 4.03, 4.16, 4.23, and 4.29 MPa, respectively. The results of the SCC-2 mix were 2.86,
532 3.68, 3.84, 3.91, and 3.95 MPa, respectively. In the three mixes, an evolution similar to
533 the compressive strength is observed. The strength reached at long-term curing suffers a
534 reduction of approximately 15% when 100% substitution of SF is carried out by NCFA,
535 and of 7% approximately when the substitution is 50% (SCC-12). Both in the SCC-2
536 and SCC-12 mixes, at an early age, there is a slightly greater difference in resistance
537 compared to the reference mix (SCC-1), which may be due, on the one hand, to the
538 larger particle size of the NCFA, which would hinder the hydration processes, as
539 already mentioned, and on the other hand, to the effect of the physical–chemical nature
540 of the filler [43].
541
542 This behaviour is in agreement with the results obtained by other authors. Esquinas et
543 al. [12] observed a decrease of approximately 18% in the splitting tensile strength of
544 SCC when the commercial SF was completely replaced by a dolomitic waste. Dehwah
545 [44] obtained superior splitting tensile strengths in SCC that incorporated silica fume
546 compared to mixes using FA, due to a higher packing density and reactivity. On the

other hand, Liu [45] obtained splitting tensile strengths similar to those achieved in this work, with SCC that used different amounts of fly ash as a substitute for cement.

Splitting tensile strength can be defined as a function of compressive strength. Figure 12 (left) shows the splitting tensile strengths of all mixes and for all ages, against compressive strength. All of them are within the limits recommended by the CEB-FIB code (Euro-International Committee of Béton - International Federation for Structural Concrete). The correlation between both parameters has been represented and expressed mathematically by Eq. 1, with $R^2$ equal to 0.85.

$$f_{ci} = 0.31 \cdot f_c^{2/3}, \qquad \text{(Eq. 1)}$$

where $f_{ci}$ is the splitting tensile strength and $f_c$ is the compressive strength.

The splitting tensile strength $f_{ci}$ can be calculated according to the EHE-08 [27] from the tensile strength, $f_{ct}$, which can be found from the characteristic compressive strength, $f_{ck}$ (Eq. 2) and taking into account Eq. 3:

$$f_{ct} = 0.3 \cdot f_{ck}^{2/3}, \qquad \text{(Eq. 2)}$$

$$f_{ci\,(EHE\text{-}08)} = f_{ct} / 0.9, \qquad \text{(Eq. 3)}$$

resulting in Eq. 4:

$$f_{ci\,(EHE\text{-}08)} = 0.33 \cdot f_{ck}^{2/3}, \qquad \text{(Eq. 4)}$$

If the concept of characteristic compressive strength ($f_{ck}$) defined by EHE-08 is used [27], Eq. 1 would be transformed into Eq. 5 ($R^2 = 0.80$).

$$f_{ci} = 0.35 \cdot f_{ck}^{2/3}, \qquad \text{(Eq. 5)}$$

Parra et al. [46] proposed Eq. 6 for its application to the SCC.

$$f_{ci\,(SCC)} = 0.28 \cdot f_c^{2/3}, \qquad \text{(Eq. 6)}$$

It can be seen that the correlation found in this work, Eq. 1, (Figure 12 left) is close to the correlation proposed by Parra et al. (Eq. 6) and very similar to that proposed by Lui [45]. On the contrary, it differs considerably from the correlation proposed by Dehwah [44], with respect to the whole range of resistances. On the other hand, if the characteristic compressive strength ($f_{ck}$) is taken into account, the correlation, Eq. 5, (Figure 12 right) is very similar to the one proposed in the EHE-08 (Eq. 4).

Table 7 lists the experimental and estimated $f_{ci}$ values according to the EHE-08 (Eq. 4), and the expression proposed by Parra et al. (Eq. 6). The calculated values are slightly lower than those obtained experimentally, as shown in Figure 12. The correlation coefficients between the experimental values and those estimated by both equations are also included. The average of the correlation coefficients between the experimental values and those obtained when applying the equation proposed by the EHE-08 (Eq. 4) was 1.06, and for the equation proposed by Parra et al. (Eq. 6), it was 1.1.

Therefore, for the dosages used in this work, the equations proposed by the EHE-08 and by Parra et al. would be valid. The equation of Parra et al. would allow prediction of the

behaviour against the splitting tensile strength in concretes that incorporate this type of waste with a slightly higher safety margin.

### 3.2.5. Flexural strength

The flexural strength of the mixes presents a similar behaviour to that of the mechanical properties analysed previously (Figure 11). For the different ages of curing (7, 28, 91, and 250 days), the flexural strength values obtained were 7.32, 8.57, 8.85, and 8.91 MPa, respectively, for the SCC-1 mix; 6.76, 8.01, 8.20, and 8.47 MPa, respectively, for the mix SCC-12; and 5.86, 7.60, 7.97, and 8.12 MPa, respectively, for the SCC-2 mix. As can be observed, during short-term curing (7 days), there is a difference between the mixes SCC-12 and SCC-2 with respect to the reference (SCC-1) of 8% and 20%, respectively. This difference is minimized with age; it was observed that for SCC-12 and SCC-2, with respect to the reference (SCC-1), the difference was 5% and 9%, respectively. As for the compressive and splitting tensile strengths, these results are clearly influenced by the characteristics of the fillers used, as discussed above, and the reactions associated with them.

Other researchers have obtained a behaviour similar to that obtained in this work. Esquinas et al. [12] observed that the flexural strength of SCC manufactured with residual filler decreased compared to that of an SCC manufactured with a commercial filler with a finer particle size distribution. On the other hand, Dehwah [44] obtained values of flexural strengths at 28 days for an SCC with FA that were lower than that for an SCC with a mix of limestone filler and silica fume, due to the greater effectiveness of the limestone filler to fill the micropores of the SCC.

The correlation between the experimental values of flexural strength and compressive strength is shown in Figure 13. This relationship is expressed by Eq. 7, where $R^2$ is equal to 0.81.

$$f_{fl} = 0.0750 \cdot f_c + 4.494, \qquad \text{(Eq. 7)}$$

where $f_{fl}$ is the flexural strength and $f_c$ is the compressive strength. As can be seen, the correlation proposed in this work differs from that proposed by Dehwah [44].

The flexural strength, $f_{ct,fl}$, [27] could be calculated from the tensile values ($f_{ct}$) by using Eq. 8:

$$f_{ct,fl} = f_{ct} \frac{1+1.5\left(\frac{h}{100}\right)^{0.7}}{1.5\left(\frac{h}{100}\right)^{0.7}}, \qquad \text{(Eq. 8)}$$

where $f_{ct}$ is the tensile strength obtained from the experimental values of splitting tensile strength by applying Eq. 3, and h is the edge of the element in mm. In Table 7, the flexural strength results, $f_{ct,fl}$, obtained by applying Eq. 8 are collected. It is observed that the experimental values are higher than the estimated values. For all ages, the correlation coefficients are greater than 1 (Table 7). Consequently, the application of the EHE-08 is clearly applicable to the SCC studied in this work, since the lower values of flexural strength estimated with respect to the experimental ones guarantee the safety of the SCC with this type of waste against bending moments.

### 3.2.6. Static elastic modulus

The results of the modulus of elasticity obtained in the three combinations for the different ages of curing (7, 28, 91, 182, and 250 days) are shown in Figure 11. The values obtained were 35.1, 38.8, 44.0, 47.9, and 49.1 GPa, respectively, for SCC-1; 28.6, 33.9, 39.3, 43.6, and 44.7 GPa, respectively, for SCC-12; and 18.8, 28.6, 35.2, 39.5, and 40.3 GPa, respectively, for SCC-2. Like the other parameters that define the mechanical behaviour of the SCC, the incorporation of this waste causes a decrease in the values of the modulus of elasticity. The differences in the values of this parameter in SCC-12 and SCC-2, with respect to SCC-1, are reduced with the setting time (8.7% in SCC-12 and 17.7% in SCC-2 at 250 curing days). This behaviour can be due to the delay in hydration and to the differences in the setting of the mixes that incorporate NCFA, as previously mentioned.

This behaviour is in agreement with other authors, such as Esquinas et al. [12], who observed the decrease of the static modulus of elasticity in SCC when replacing the commercial SF with dolomitic waste. The authors related it to a thicker particle size distribution of the by-product that originated a more porous structure [11], as well as to the pozzolanic characteristics of the SF. In the present work, NCFA presents a larger particle size distribution, which will hinder the development of pozzolanic reactions and will lead to lower values of the modulus of elasticity. On the other hand, Silva and Brito [42] observed an increase in the values of this parameter in mixes with FA compared to those that incorporated limestone filler due to the joint action of the smaller particle size of the FA and its pozzolanic capacity.

Figure 14 shows the relationship between the experimental values of the modulus of elasticity and the compressive strength for ages greater than 28 days expressed by Eq. 9, where $R^2$ is equal to 0.94:

$$E_{cm} = 1.79 \cdot f_c^{0.8}, \qquad \text{(Eq. 9)}$$

where $f_c$ is the compressive strength and $E_{cm}$ is the modulus of elasticity. The correlation is within the estimates of the CEB-FIB code.

The modulus of elasticity, $E_{cm}$, at 28 days, can be calculated from the average compressive strength of concrete at 28 days ($f_{cm}$) using Eq. 10 proposed by the EHE-08 [27].

$$E_{cm} = \alpha \cdot 8{,}500 \sqrt[3]{f_{cm}}, \qquad \text{(Eq.10)}$$

Eq. 10 is valid as long as the stresses, under service conditions, do not exceed the value of 0.40 $f_{cm}$. For the modulus of elasticity at different ages to 28 days, the EHE-08 proposes Eq. 11, since the growth of the module with age is different from that experienced by compressive strength.

$$E_{cm}(t) = (f_{cm}(t) / f_{c,m})^{0.3} \cdot E_{cm,} \qquad \text{(Eq. 11)}$$

where α is the correction coefficient as a function of the nature of the aggregates (in this article, the value of α is 1, because they are concretes manufactured with aggregates of medium characteristics of quartzite type), $E_{cm}(t)$ is the modulus of elasticity at t days,

$E_{cm}$ is the modulus of elasticity at 28 days, $f_{cm}(t)$ is the average compressive strength at t days, and $f_{cm}$ is the average compressive strength at 28 days.

Figure 14 includes the correlations established by other authors such as the EHE-08, Silva and Brito [42], and Felekoglu et al. [47], to compare with the data obtained in this work. The equation proposed by Felekoglu et al. has a similar slope, although the values are slightly lower for the same compressive strength, which could be due to the lower content of coarse aggregate (600 kg/m$^3$ vs 800 kg/m$^3$) and the inert addition (limestone filler) used by these authors.

Table 7 presents the modulus elasticity values estimated by the expressions proposed by the EHE-08 (Eqs. 10 and 11). It is observed that the estimated values are lower than the experimental values. The correlation factor is close to 1.2, demonstrating the validity of the Spanish instruction EHE-08 for SCCs.

In summary, all the mixes that incorporate NCFA as a filler reach values of modulus of elasticity higher than 40 GPa for long age of curing, fulfilling the requirements specified by the EHE-08, with respect to the elastic deformations under normal tensions.

### 3.2.7. UPV test

This non-destructive test allows indirect determination of the strength presented by the SCC. The UPV depends on the compactness and density of the mixes [48]. The UPV values obtained were 4.76, 4.92, 4.95, 5.01, and 5.07 km/s in SCC-1; 4.67, 4.88, 4.84,

4.96, and 5.02 km/s in SCC-12; and 4.60, 4.77, 4.82, 4.87, and 4.95 km/s in SCC-2, for 7, 28, 91, 182, and 250 days, respectively. The UPV increases with the age of curing in the three mixes, highlighting the values obtained in SCC-1 compared to SCC-12 and SCC-2. This increase in the velocity of propagation coincides with the higher values of compressive strength.

Figure 15 shows a good correlation ($R^2 = 0.89$) between the velocity of propagation and the compressive strength and can be expressed by Eq. 12:

$$UPV = 0.0119 \cdot f_c + 4.3211, \quad \text{(Eq. 12)}$$

where UPV is the ultrasonic pulse velocity and $f_c$ is the compressive strength. The correlation proposed by Dehwah [44] differs markedly from the experimental results of this work. On the contrary, the correlation proposed by Liu [45] is considerably close.

The decrease in UPV observed with decreasing compactness and density of the mixes is similar to that reported by other authors for SCCs using different wastes [12, 45, 49]. Liu [45] used fly ash as a filler and obtained UPV values of the same order as those recorded in this work.

Finally, all the mixes can be considered excellent according to the classification carried out by Whitehurst [50], since they present values higher than 4.5 km/s.

### 3.2.8. Shrinkage

The shrinkage values obtained in the different SCCs were -111, -162, -226, and -322 μstrain in SCC-1; -100, -155, -216, and -312 μstrain in SCC-12; and -83, -131, -185, and -291 μstrain in SCC-2; at 7, 14, 28, and 91 days, respectively (Table 8). Therefore, the mix with the highest shrinkage is the SCC-1 mix followed by the SCC-12 and SCC-2 mixes. This behaviour can be due to the greater chemical and autogenous shrinkage that SCC-1 presents due to the more intense pozzolanic reactions generated by the SF with respect to the other fillers NCFA + SF (SCC-12) or NCFA (SCC-2). This dimensional variation will be produced both by the development of the initial hydration reactions and by the forces of attraction that occur in the walls of the capillaries when the water retained in the porous structure is used (self-desiccation) to generate the reactions of hydration [50-52].

This is in agreement with the results obtained by Esquinas et al. [12], who observed a decrease in the shrinkage in the mixes that incorporated a dolomitic residual powder with a larger size distribution than the SF used in the reference mix, in which a greater shrinkage was observed, and was attributed to the greater reactivity of the SF. In this same sense, Guneyisi et al. [53] observed higher values of shrinkage in the mixes that incorporated silica fume compared to those that incorporated FA due to their larger particle size.

It can be concluded that the SCCs that incorporate NCFA as a filler, SCC-12 and SCC-2, perform better than SCC-1, in relation to shrinkage at an early age, which would result in less cracking by the initial deformation due to these phenomena.

## 4. Conclusions

A comparative study of three SCC mixes was carried out to evaluate an NCFA-like filler in SCC; in the first mix (SCC-1), a commercial SF was used as a reference; in the second (SCC-12) a mix, 1:1 in volume, of SF and NCFA was used; and in the third (SCC-2), only NCFA was used.

The self-compactability tests show reproducibility. All mixes accomplish with the parameters stipulated by the EHE-08.

The densities of SCC-12 (2.421 kg/dm$^3$) and SCC-2 (2.397 kg/dm$^3$) in the fresh state are slightly less than that of SCC-1 (2.441 kg/dm$^3$), and this is related to the finer and continuous particle size distribution of the SF with respect to the NCFA.

The thermogravimetric study shows that in SCC-1, the higher weight loss occurs in the dehydration zone (0–400 ºC); in SCC-2, it occurs in the decarbonation area (550–750 ºC). It can be concluded that the setting mechanism of both concretes (SCC-1 and SCC-2) is different, depending on the nature of filler added. In the case of the SCC-12 mix, the behaviour is intermediate. In short, pozzolanic and mild carbonation reactions occur in the SCC-1 mix. In the SCC-12 mix, both pozzolanic and carbonation reactions are observed. In the SCC-2 mix, only carbonation processes are observed.

The three mixes have similar wet density values (measured at 28 days), although slightly lower for the mixes that incorporate NCFA: 2.418 kg/dm$^3$ (SCC-12) and 2.398 kg/dm$^3$ (SCC-2) compared to the mix of references 2.438 kg/dm$^3$ (SCC-1). The dry densities follow the same pattern as that observed in the case of wet densities: 2.329

796 kg/dm$^3$, 2.323 kg/dm$^3$, and 2.284 kg/dm$^3$ for SCC-1, SCC-12, and SCC-2 mixes,
797 respectively.
798
799 The compressive strength, splitting tensile strength, flexural strength, and static
800 modulus of elasticity of SCCs produced with NCFA (SCC-12 and SCC-2) are lower
801 than those of the SCC produced with SF (SCC-1), for all ages. The differences were
802 higher at an early age.
803
804 The delay in hydration observed in these mixes may be due to the greater particle size
805 distribution of the NCFA, (45% of the particles are greater than 32 μm versus 12% in
806 the SF), making the complete hydration of the particles and therefore the mechanical
807 development difficult.
808
809 The splitting tensile strength, flexural strength, and static modulus of elasticity values
810 calculated using the EHE-08 are lower than those obtained experimentally, i.e., the
811 correlation ratios are in most cases greater than 1. Hence, the experimental results show
812 the validity of using the EHE-08, initially proposed for normally vibrated concrete
813 (NVC), in SCC.
814
815 There is an increase in the UPV relative to the curing age and the values for all mixes,
816 and this can be attributed to the increase in compacity and compressive strength. The
817 mixes can be considered excellent since they present UPV values higher than 4.5 km/s.
818
819 The incorporation of NCFA as a filler in SCCs, SCC-12, and SCC-2 resulted in their
820 better performance than SCC-1 in relation to shrinkage at an early age, which would

result in less cracking by the initial deformation due to these phenomena.

One may conclude therefore, that it is possible to obtain an SCC, by replacing (in volume) a natural SF with NCFA from coal-fired power plants to achieve a mechanical behaviour greater than the minimum levels stipulated by the Spanish Code on Structural Concrete (EHE-08).

## Acknowledgments

This work was partly supported by the Andalusian Regional Government (Research Groups FQM-391 and TEP-227). A. Romero Esquinas also acknowledges funding from MECD-Spain (http://www.mecd.gob.es/educacion-mecd/) FPU-13/04030. The authors wish to thank the Research Plan of the University of Córdoba (2016), the staff at the Electron Microscopy and Elemental Analysis units of the Central Research Support Service (SCAI) of University of Córdoba for their technical assistance, the Fine Chemistry Institute of the University of Córdoba for their technical support, BASF Chemical Company for supplying the admixture, and Portland Valderrivas (Alcalá de Guadaira, Seville) for the supplied cement. The authors wish to thank the Andalusian Innovation Centre for Sustainable Construction (CIAC) for the use of the press IBERTEST, model MEH-3000. The authors wish to thank the National Radioactive Waste Company (ENRESA) for Contract of Research 079000146. Finally, the authors wish to thank the Puente Nuevo Coal-fired Power Plant of company Viesgo for the supplied NCFA waste.

## References

[1] European Commission, Report from the commission to the European parliament, the council, the European Economic and Social Committee and the Committee of the Regions on the Implementation of the Circular Economy Action Plan, (2017).

[2] K. Celik, C. Meral, A.P. Gursel, P.K. Mehta, A. Horvath, P.J. Monteiro, Mechanical properties, durability, and life-cycle assessment of self-consolidating concrete mixtures made with blended portland cements containing fly ash and limestone powder, Cement and Concrete Composites 56 (2015) 59-72.

[3] J. Moya, N. Pardo, A. Mercier, Energy efficiency and $CO_2$ emissions: Prospective scenarios for the Cement industry, Publications Office2010.

[4] H. Okamura, Self-compacting high-performance concrete, Concrete international 19(7) (1997) 50-54.

[5] Asociación Cientifico Técnica del Hormigón Estructural (ACHE). M-13: Hormigón Autocompactante. Diseño y Aplicación; 2008.

[6] European Federation of National Associations Representing producers and applicators of specialist building products for Concrete (EFNARC). Specification and guidelines for self-compacting concrete, Hampshire, UK; 2002, www.efnarc.org.

[7] European Federation of National Associations Representing producers and applicators of specialist building products for Concrete (EFNARC). The European guidelines for self-compacting concrete specification. Production and Use. Hampshire, UK; (2005), www.efnarc.org.

[8] R. Sharma, R.A. Khan, Durability assessment of self compacting concrete incorporating copper slag as fine aggregates, Construction and Building Materials 155 (2017) 617-629.

867 [9] S. Subaşı, H. Öztürk, M. Emiroğlu, Utilizing of waste ceramic powders as filler
868 material in self-consolidating concrete, Construction and Building Materials 149 (2017)
869 567-574.
870 [10] M. Gesoglu, E. Güneyisi, O. Hansu, S. Etli, M. Alhassan, Mechanical and fracture
871 characteristics of self-compacting concretes containing different percentage of plastic
872 waste powder, Construction and Building Materials 140 (2017) 562-569.
873 [11] A. Esquinas, J. Álvarez, J. Jiménez, J. Fernández, J. de Brito, Durability of self-
874 compacting concrete made with recovery filler from hot-mix asphalt plants,
875 Construction and Building Materials 161 (2018) 407-419.
876 [12] A.R. Esquinas, C. Ramos, J. Jiménez, J. Fernández, J. de Brito, Mechanical
877 behaviour of self-compacting concrete made with recovery filler from hot-mix asphalt
878 plants, Construction and Building Materials 131 (2017) 114-128.
879 [13] A.S. Gill, R. Siddique, Strength and micro-structural properties of self-compacting
880 concrete containing metakaolin and rice husk ash, Construction and Building Materials
881 157 (2017) 51-64.
882 [14] N. Ranjbar, A. Behnia, B. Alsubari, P.M. Birgani, M.Z. Jumaat, Durability and
883 mechanical properties of self-compacting concrete incorporating palm oil fuel ash,
884 Journal of Cleaner Production 112 (2016) 723-730.
885 [15] J. Cuenca, J. Rodríguez, M. Martín-Morales, Z. Sánchez-Roldán, M. Zamorano,
886 Effects of olive residue biomass fly ash as filler in self-compacting concrete,
887 Construction and Building Materials 40 (2013) 702-709.
888 [16] Asociación Española de Normalización y Certificación, AENOR, Madrid, Spain,
889 (2018).
890 [17] American Society of Testing Materials, ASTM International, West Conshohocken,
891 USA, (2018).

892 [18] P. Da Silva, J. De Brito, Experimental study of the porosity and microstructure of
893 self-compacting concrete (SCC) with binary and ternary mixes of fly ash and limestone
894 filler, Construction and Building Materials 86 (2015) 101-112.
895 [19] S. Dadsetan, J. Bai, Mechanical and microstructural properties of self-compacting
896 concrete blended with metakaolin, ground granulated blast-furnace slag and fly ash,
897 Construction and Building Materials 146 (2017) 658-667.
898 [20] G. Sua-iam, N. Makul, Incorporation of high-volume fly ash waste and high-
899 volume recycled alumina waste in the production of self-consolidating concrete, Journal
900 of Cleaner Production 159 (2017) 194-206.
901 [21] K. Celik, M.D. Jackson, M. Mancio, C. Meral, A.-H. Emwas, P.K. Mehta, P.J.M.
902 Monteiro, High-volume natural volcanic pozzolan and limestone powder as partial
903 replacements for portland cement in self-compacting and sustainable concrete, Cement
904 and concrete composites 45 (2014) 136-147.
905 [22] A.I. Torres-Gómez, E.F. Ledesma, R. Otero, J.M. Fernández, J.R. Jiménez, J. de
906 Brito, Combined Effects of Non-Conforming Fly Ash and Recycled Masonry
907 Aggregates on Mortar Properties, Materials 9(9) (2016) 729.
908 [23] A. Niyogi, Characterization of fly ash fractions to trace the extent of pollution,
909 2017 World of Coal Ash (WOCA) Conference in Lexington (2017),
910 http://wwwflyash.info.
911 [24] European Coal Combustion Products Association (ECOBA). Available online:
912 http://www.ecoba.com/ecobaccpprod.html.
913 [25] International Energy Outlook 2017, U.S. Energy Information Administration, EIA
914 (2017). http://wwweia.gov/ieo.
915 [26] Directive 2008/98/EC of the European Parliament and of the Council of 10
916 November 2008 onWaste. Official Journal of the European Union. 2008.

917 [27] EHE-08. Spanish Structural Concrete Code EHE-08 [Instrucción de Hormigón
918 Estructural EHE-08]. R.D. 1247/2008, Spain (2008).
919 [28] P. Swarthmore, Joint Committee on Power Diffraction Standard-International
920 Centre for Diffraction Data. (1995).
921 [29] J.M. Pommersheim, Effect of particle size distribution on hydration kinetics, MRS
922 Proceedings, Cambridge Univ Press, 1986, p. 301.
923 [30] S. Tsivilis, S. Tsimas, A. Benetatou, E. Haniotakis, Study on the contribution of the
924 fineness on cement strength, (1990).
925 [31] D.P. Bentz, E.J. Garboczi, C.J. Haecker, O.M. Jensen, Effects of cement particle
926 size distribution on performance properties of Portland cement-based materials, Cement
927 and Concrete Research 29(10) (1999) 1663-1671.
928 [32] M. Fernández Cánovas, Hormigón, Ed. Colegio de Ingenieros de Caminos, Canales
929 y Puertos (2007).
930 [33] V. Kocaba, Development and evaluation of methods to follow microstructural
931 development of cementitious systems including slags, in, EPFL, 2009.
932 [34] S. Brunauer, P.H. Emmett, E. Teller, Adsorption of gases in multimolecular layers,
933 Journal of the American chemical society 60(2) (1938) 309-319.
934 [35] A.W. Saak, Characterization and modeling of the rheology of cement paste: with
935 applications toward self-flowing materials, 2000.
936 [36] P.R.d. Silva, J.d. Brito, Fresh-state properties of self-compacting mortar and
937 concrete with combined use of limestone filler and fly ash, Materials Research 18(5)
938 (2015) 1097-1108.
939 [37] I.B. Topcu, T. Bilir, T. Uygunoğlu, Effect of waste marble dust content as filler on
940 properties of self-compacting concrete, Construction and Building Materials 23(5)
941 (2009) 1947-1953.

[38] S. Barbhuiya, Effects of fly ash and dolomite powder on the properties of self-compacting concrete, Construction and Building Materials 25(8) (2011) 3301-3305.

[39] J. Gibbs, W. Zhu, Strength of hardened self-compacting concrete, Proceedings of First international RILEM Symposium on Self-Compacting Concrete (PRO 7), Stockholm, Suede, 1999, pp. 199-209.

[40] F. Puertas, T. Vázquez, Early hydration cement Effect of admixtures superplasticizers, Materiales de construcción 51(262) (2001) 53-61.

[41] Fernández Rodríguez J.M., "Introducción a los Cementos", Servicio de Publicaciones Universidad de Córdoba (2004), ISBN 84-7801-731-3.

[42] P. Silva, J. de Brito, Experimental study of the mechanical properties and shrinkage of self-compacting concrete with binary and ternary mixes of fly ash and limestone filler, European Journal of Environmental and Civil Engineering 21(4) (2017) 430-453.

[43] P. Domone, A review of the hardened mechanical properties of self-compacting concrete, Cement and Concrete Composites 29(1) (2007) 1-12.

[44] H. Dehwah, Mechanical properties of self-compacting concrete incorporating quarry dust powder, silica fume or fly ash, Construction and building materials 26(1) (2012) 547-551.

[45] M. Liu, Self-compacting concrete with different levels of pulverized fuel ash, Construction and Building Materials 24(7) (2010) 1245-1252.

[46] C. Parra, M. Valcuende, F. Gomez, Splitting tensile strength and modulus of elasticity of self-compacting concrete, Construction and Building materials 25(1) (2011) 201-207.

[47] B. Felekoğlu, S. Türkel, B. Baradan, Effect of water/cement ratio on the fresh and hardened properties of self-compacting concrete, Building and Environment 42(4) (2007) 1795-1802.

967 [48] G. Trtnik, F. Kavčič, G. Turk, Prediction of concrete strength using ultrasonic
968 pulse velocity and artificial neural networks, Ultrasonics 49(1) (2009) 53-60.
969 [49] M. Uysal, K. Yilmaz, Effect of mineral admixtures on properties of self-
970 compacting concrete, Cement and Concrete Composites 33(7) (2011) 771-776.
971 [50] E.A. Whitehurst, Soniscope tests concrete structures, Journal Proceedings, 1951,
972 pp. 433-444.
973 [51] A.P.M. Šahinagić-Isović, M. Šahinagić-Isović, G. Markovski, M. Ćećez, Shrinkage
974 strain of concrete-causes and types, Građevinar 64(09.) (2012) 727-734.
975 [52] M. Valcuende, F. Benito, C. Parra, I. Miñano, Shrinkage of self-compacting
976 concrete made with blast furnace slag as fine aggregate, Construction and Building
977 Materials 76 (2015) 1-9.
978 [53] E. Güneyisi, M. Gesoğlu, E. Özbay, Strength and drying shrinkage properties of
979 self-compacting concretes incorporating multi-system blended mineral admixtures,
980 Construction and Building Materials 24(10) (2010) 1878-1887.
981

982 **Figure captions**

983 Figure 1. Particle size distribution for gravel, coarse, and fine sands, mixes SCC-1,
984 SCC-12, and SCC-2.
985 Figure 2. PXRD patterns for gravel (G), coarse (S1), and fine (S2) sands.
986 Figure 3. Grain-size distribution of SF, NCFA, and CEM I by laser diffraction.
987 Figure 4. PXRD patterns for SF, NCFA, and cement.
988 Figure 5. TG (solid lines) and DTA (dotted line) curves for the SF and NCFA fillers.
989 Figure 6. Pore size distribution for the SF and NCFA fillers.
990 Figure 7. Workability boxes for several self-compacting mixes.
991 Figure 8. TGA (solid lines) and TDA (dotted lines) for several hardened SCCs.
992 Figure 9. PXRD patterns for hardened SCC-1 and SCC-2 in the short term.

993 Figure 10. PXRD patterns for hardened SCC-1, SCC-12 and SCC-2 at 250 days.

994 Figure 11. Mechanical properties of hardened SCCs.

995 Figure 12. Compressive strength (fc) versus splitting tensile strength (left) and

996 compressive strength (fck) versus splitting tensile strength (right).

997 Figure 13. Compressive strength versus flexural strength.

998 Figure 14 Compressive strength versus modulus of elasticity.

999 Figure 15. Compressive strength versus ultrasonic pulse velocity.

1000

1001

# TABLES

Table 1. Characterisation of aggregates.

| **Characteristic** | **Standard** | **G** | **S1** | **S2** | **Limit set by EHE-08** |
|---|---|---|---|---|---|
| Size (mm) | UNE-EN 933-1 | 4/16 | 0/4 | 0/2 | <25 |
| Fines content (%) [(a)] | UNE-EN 933-1 | 0.2 | 1 | 1 | <8 |
| Index slabs (%) | UNE-EN 933-3 | 10.3 | - | - | < 35 |
| Crushed and broken surfaces (%) | UNE-EN 933-5 | 86 | - | - | Not limited |
| Los Angeles coefficient | UNE-EN 1097-2 | 18 | - | - | ≤ 40 |
| Dry sample density $\rho_{rd}$ ($g/cm^3$) | UNE-EN 1097-6 | 2.62 | 2.63 | 2.66 | Not limited |
| Water absorption (%) | UNE-EN 1097-6 | 0.73 | 0.49 | 0.33 | ≤ 5 |
| Friability coefficient (%) | UNE 83115 | - | 17.3 | 18 | < 40 [(b)] |
| Surface cleaning (%) | UNE 146130 | 0.05 | - | - | Not limited |
| Water soluble chlorides (% Cl) | UNE-EN 1744-1 | $6 \times 10^{-4}$ | $6 \times 10^{-4}$ | $1.4 \times 10^{-3}$ | ≤ 0.03 |
| Acid soluble sulphates (% $SO_3$) | UNE-EN 1744-1 | $9 \times 10^{-3}$ | $2 \times 10^{-2}$ | $4 \times 10^{-3}$ | ≤ 0.8 |
| Water soluble sulphates (% $SO_3$) | UNE-EN 1744-1 | $2 \times 10^{-2}$ | $7 \times 10^{-3}$ | $2 \times 10^{-2}$ | ≤ 0.8 |
| Sulphur content (%) | UNE-EN 1744-1 | ND [(c)] | ND | ND | ≤ 1 |
| Organic matter content (%) | UNE-EN 1744-1 | 0.05 | 0.13 | 0.12 | ≤ 1 [(d)] - ≤ 0.5 [(e)] |

[(a)] Finer than 0.063 mm; [(b)] Recommendation; [(c)] ND: No Detected; [(d)] Coarse aggregates; [(e)] Fine aggregates

Table 2. Characterisation of filler and cement.

| **Characteristic** | **Standard** | **SF** | **NCFA** | **Cement** | **G** | **S1** | **S2** |
|---|---|---|---|---|---|---|---|
| $SiO_2$ % | - | 100 | 28.50 | 13.30 | 65.98 | 52.95 | 59.85 |
| $Al_2O_3$ % | - | - | 54.90 | 6.60 | 13.10 | 17.33 | 15.30 |
| $Fe_2O_3$ % | - | - | 14.90 | 16.60 | 9.18 | 15.62 | 13.10 |
| $SO_3$ % | - | - | - | 5.00 | - | - | - |
| CaO % | - | - | 0.60 | 56.30 | 5.02 | 5.01 | 4.95 |
| MgO % | - | - | 0.60 | 0.70 | 0.48 | 0.44 | 0.40 |
| $Na_2O$% | - | - | - | - | 1.64 | 2.63 | 1.80 |
| $K_2O$% | - | - | - | - | 4.59 | | |
| Other | - | - | 0.50 | 1.50 | - | - | - |
| Particle size > 32 μm (%) | - | 17.13 | 15.35 | 13.66 | - | - | - |
| Particle size 3 - 32 μm (%) | - | 71.28 | 39.64 | 59.96 | - | - | - |
| Particle size < 3 μm (%) | - | 11.59 | 45.01 | 26.38 | - | - | - |
| BET surface area ($m^2/g$) | - | 2.90 | 1.80 | 0.67 | - | - | - |
| Particle density $_{(}g/cm^3$) | UNE 80103 | 2.60 | 1.86 | 3.10 | - | - | - |
| Bulk density ($g/cm^3$) | UNE-EN 1097-3 | 0.69 | 1.04 | - | - | - | - |

Table 3. Concrete mix proportions and dosing tests.

| **Mixes** | **SCC-1** | | | | **SCC-12** | | | | **SCC- 2** | | | |
|---|---|---|---|---|---|---|---|---|---|---|---|---|
| | Dry weight | | *Volume* | | Dry weight | | *Volume* | | Dry weight | | *Volume* | |
| **Constituent** | Kg/m$^3$ | % | *Liters* | *%* | Kg/m$^3$ | % | *Liters* | *%* | Kg/m$^3$ | % | *Liters* | *%* |
| **Gravel 4/16 (G)** | 807.65 | 33.05 | *309.80* | *30.26* | 797.81 | 32.97 | *306.03* | *29.89* | 789.07 | 32.79 | *302.67* | *29.56* |
| **Sand 0/4 (S1)** | 657.28 | 26.90 | *250. 59* | *24.47* | 649.28 | 26.83 | *247.53* | *24.17* | 642.16 | 26.69 | *244.82* | *23.91* |
| **Sand 0/2 (S2)** | 280.82 | 11.49 | *106.33* | *10.38* | 284.37 | 11.75 | *107.68* | *10.52* | 300.82 | 12.50 | *111.91* | *11.12* |
| **Filler (SF)** | 101.75 | 4.16 | *39.13* | *3.82* | 51.96 | 2.15 | *19.99* | *1.95* | 0.00 | 0.00 | *0.00* | *0.00* |
| **Filler (NCFA)** | 0.00 | 0.00 | *0.00* | *0.00* | 41.57 | 1.72 | *22.30* | *2.18* | 72.94 | 3.03 | 39.13 | 3.82 |
| **Cement** | 410.00 | 16.78 | *132.26* | *12.92* | 410.00 | 16.94 | *132.26* | *12.92* | 410.00 | 17.04 | *132.26* | *12.92* |
| **Superplasticizer** | 9.21 | 0.38 | *8.90* | *0.87* | 9.06 | 0.37 | *8.76* | *0.86* | 8.69 | 0.36 | *8.40* | *0.82* |
| **Water** | 176.93 | 7.24 | *176.93* | *17.28* | 179.40 | 7.40 | *179.40* | *17.52* | 182.75 | 7.59 | *182.75* | *17.85* |
| | **Glenium 303SCC** | | | | **Glenium 303SCC** | | | | **Glenium 303SCC** | | | |
| **(W/C) $_{total}$** | 0.432 | | | | 0.437 | | | | 0.446 | | | |
| **(W/C) $_{ef}$** | 0.422 | | | | 0.428 | | | | 0.436 | | | |

| | **Typical range**[a] | SCC-1 | SCC-12 | SCC-2 |
|---|---|---|---|---|
| Coarse aggregate (kg/m$^3$) | 750-1000 | 807.65 | 797.81 | 789.07 |
| Fine aggregate (sand) (%) | 48-55[b] | 53.5 | 53.7 | 54.2 |
| Fines (kg/m$^3$) / [L/m$^3$] | 380-600[d] | 544.52 / [183.87] | 519.98 / [177.95] | 486.46 / [168.13] |
| Water (litres/m$^3$) | 150-210 | 176.93 | 179.40 | 182.75 |
| Paste (litres/m$^3$) | 300-380 | 360.80 | 357.35 | 350.89 |
| Water/fines [c] | 0.85-1.10 | 0.96 | 1.01 | 1.09 |

[a] EFNARC dosage parameters [7] [b] Volume total weight of aggregate in balanced quintiles. % of sand S1and S2 relative to the whole of the aggregates. [c] by volume. [d] kg/m$^3$

Table 4. Self-compactability tests.

| **Test** | **Characteristics evaluated** | **Standard** | **Parameters** | **Admissible values** [27] |
|---|---|---|---|---|
| Slump flow test | Unobstructed filling ability | UNE-EN 12350-8 | $d_f$ = final flow diameter | 550 mm ≤ $d_f$ ≤ 850 mm |
| | Resistance to segregation [(a)] | | $T_{50}$ = time spent to reach the 500 mm | $T_{50}$ ≤ 8s |
| J-Ring test | Passing ability | UNE-EN 12350-12 | $d_{jf}$ = final flow diameter | ≥ $d_f$ - 50 mm |
| | Resistance to segregation [(a)] | | | |
| V-funnel test | Filling ability | UNE-EN 12350-9 | Tv = funnel flow time | 4 s ≤ Tv ≤ 20 s |
| | Passing ability | | | |
| L-box test | Passing ability | UNE-EN 12350-10 | $C_{bL}$ = blocking coefficient | 0.75 ≤ $C_{bl}$ ≤ 1 |
| | Resistance to segregation [(a)] | | | |

[(a)] No standardized

Table 5. Results of the self-compactability tests for the two types of SCC.

| **Mixtures** | **Retakes** | **Slump flow test** | | **J-Ring test** | | **V-funnel test** | **L-box test** |
|---|---|---|---|---|---|---|---|
| | | $T_{50}$ (s) | $d_f$ (mm) | $T_{j50}$ (s) | $d_f - d_{jf}$ | $T_v$ (s) | $C_{bL}$ |
| **SSC-1** | Average (SD) [(a)] | 2.34 (0.2) | 725.13 (6.1) | 3.06 (0.6) | 38 (2.5) | 7.13 (0.4) | 0.92 (0.02) |
| *Class* [27] | | *AC-V2* | *AC-E2* | | *AC-RB2* | *AC-V2* | *AC-RB2* |
| **SSC-12** | Average (SD) [(a)] | 4.35 (0.1) | 699 (4.53) | 5.56 (0.4) | 25 (3.2) | 10.07 (0.4) | 0.82 (0.01) |
| *Class* [27] | | *AC-V1* | *AC-E2* | | *AC-RB2* | *AC-V1* | *AC-RB2* |
| **SSC-2** | Average (SD) [(a)] | 2.69 (0.3) | 676.75 (4.3) | 3.67 (0.4) | 24 (5.3) | 11.10 (0.5) | 0.84 (0.04) |
| *Class* [27] | | *AC-V1* | *AC-E2* | | *AC-RB2* | *AC-V1* | *AC-RB2* |

[(a)] Standard deviation

Table 6. Results obtained in the test of thermal analysis (TG/TD) for each SCC studied.

| **Mixtures** | **Age (days)** | **Δ mass (%)** | | | | **Chemical species (kg/m$^3$)** | | | | |
|---|---|---|---|---|---|---|---|---|---|---|
| | | **0-400ºC** | **400-550ºC** | **550-750ºC** | **750-800ºC** | **$H_2O_{Total}$** | **$Ca(OH)_2$** | **$CaCO_3$** | **$CaCO_3$[(a)]** | **$Ca(OH)_{2\ Total}$** |
| **SCC-1** | 28 | -1.3828 | -0.6951 | -3.2415 | -0.0881 | 33.8 | 69.9 | 21.1 | 159.0 | 85.5 |
| | 91 | -2.2919 | -0.8090 | -3.2848 | -0.1718 | 56.0 | 81.3 | 23.5 | 159.0 | 98.7 |
| | 250 | -4.5444 | -0.8407 | -3.2981 | -0.0884 | 111.0 | 84.5 | 24.3 | 159.0 | 102.5 |
| **SCC-12** | 28 | -1.2132 | -0.7121 | -3.3400 | -0.0584 | 29.4 | 71.0 | 25.0 | 159.0 | 89.5 |
| | 91 | -1.8944 | -0.6784 | -3.5102 | -0.0300 | 45.9 | 67.6 | 34.0 | 159.0 | 93.1 |
| | 250 | -3.1612 | -0.8999 | -3.6453 | -0.1642 | 76.6 | 89.7 | 42.0 | 159.0 | 120.7 |
| **SCC-2** | 28 | -1.1867 | -0.5581 | -3.2068 | -0.0697 | 28.6 | 55.2 | 16.5 | 159.0 | 67.4 |
| | 91 | -1.4592 | -0.7625 | -3.2762 | -0.0868 | 35.1 | 75.5 | 20.3 | 159.0 | 90.5 |
| | 250 | -2.5542 | -0.9789 | -3.9001 | -0.0890 | 61.5 | 96.9 | 54.0 | 159.0 | 137.2 |

[(a)] Amount $CaCO_3$ present on aggregates.

Table 7. Comparing the experimental results with those estimated using EHE-08 and other references.

| Mixtures | Age (days) | Experimental | | | Estimated by EHE-08 | | | Parra[(a)] | Correlation ratio | | | |
|---|---|---|---|---|---|---|---|---|---|---|---|---|
| | | $f_{ci}$ (MPa) | $f_{ct,fl}$ (MPa) | $E_{cm}$ (GPa) | $f_{ci}$ (MPa) | $f_{ct,fl}$ (MPa) | $E_{cm}$ (GPa) | $f_{ci}$ (MPa) | $f_{ci(EHE)}$ | $f_{ct,fl(EHE)}$ | $E_{cm(EHE)}$ | $f_{ci(SCC)}$ |
| **SCC-1** | 7 | 3.51 | 7.32 | 35.1 | 3.41 | 5.27 | - | 2.86 | 1 | 1.3 | - | 1.1 |
| | 28 | 4.42 | 8.57 | 38.8 | 4.05 | 6.63 | 31.4 | 3.40 | 1.1 | 1.2 | 1.2 | 1.1 |
| | 91 | 4.57 | 8.85 | 44.0 | 4.46 | 6.86 | 32.6 | 3.74 | 1 | 1.2 | 1.3 | 1.1 |
| | 182 | 4.63 | - | 47.9 | 4.76 | - | 33.4 | 4.00 | 1 | - | 1.3 | 1.1 |
| | 250 | 4.67 | 8.91 | 49.0 | 4.96 | 7.00 | 33.9 | 4.16 | 0.9 | 1.2 | 1.3 | 1 |
| **SCC-12** | 7 | 3.16 | 6.76 | 28.6 | 2.91 | 4.74 | - | 2.45 | 1.1 | 1.3 | - | 1.1 |
| | 28 | 4.03 | 8.01 | 33.9 | 3.45 | 6.05 | 29.4 | 2.90 | 1.1 | 1.2 | 1.1 | 1.2 |
| | 91 | 4.16 | 8.20 | 39.3 | 3.83 | 6.24 | 30.5 | 3.22 | 1.1 | 1.3 | 1.2 | 1.1 |
| | 182 | 4.23 | - | 43.6 | 4.16 | - | 31.5 | 3.49 | 1 | - | 1.3 | 1.1 |
| | 250 | 4.29 | 8.47 | 44.7 | 4.38 | 6.43 | 32.1 | 3.68 | 1 | 1.2 | 1.3 | 1.1 |
| **SCC-12** | 7 | 2.86 | 5.86 | 18.8 | 2.46 | 4.24 | - | 2.06 | 1.1 | 1.3 | | 1.1 |
| | 28 | 3.68 | 7.60 | 28.6 | 3.05 | 5.53 | 28.0 | 2.56 | 1.2 | 1.3 | 1 | 1.2 |
| | 91 | 3.84 | 7.97 | 35.2 | 3.41 | 5.77 | 29.1 | 2.86 | 1 | 1.3 | 1.2 | 1.1 |
| | 182 | 3.95 | - | 39.5 | 3.75 | - | 30.1 | 3.15 | 1 | - | 1.2 | 1.1 |
| | 250 | 3.66 | 8.12 | 40.3 | 3.95 | 5.93 | 30.7 | 3.32 | 1 | 1.3 | 1.2 | 1.1 |

[(a)] (Eq. 6)

Table 8. Total shrinkage.

| | Age (days) | SCC-1 | SCC-12 | SCC-2 |
|---|---|---|---|---|
| Total shrinkage strain (μ) | 7 | -111 | -100 | -83 |
| | 14 | -162 | -155 | -131 |
| | 28 | -226 | -216 | -185 |
| | 91 | -322 | -312 | -291 |

Figure
Click here to download Figure: Figures.docx

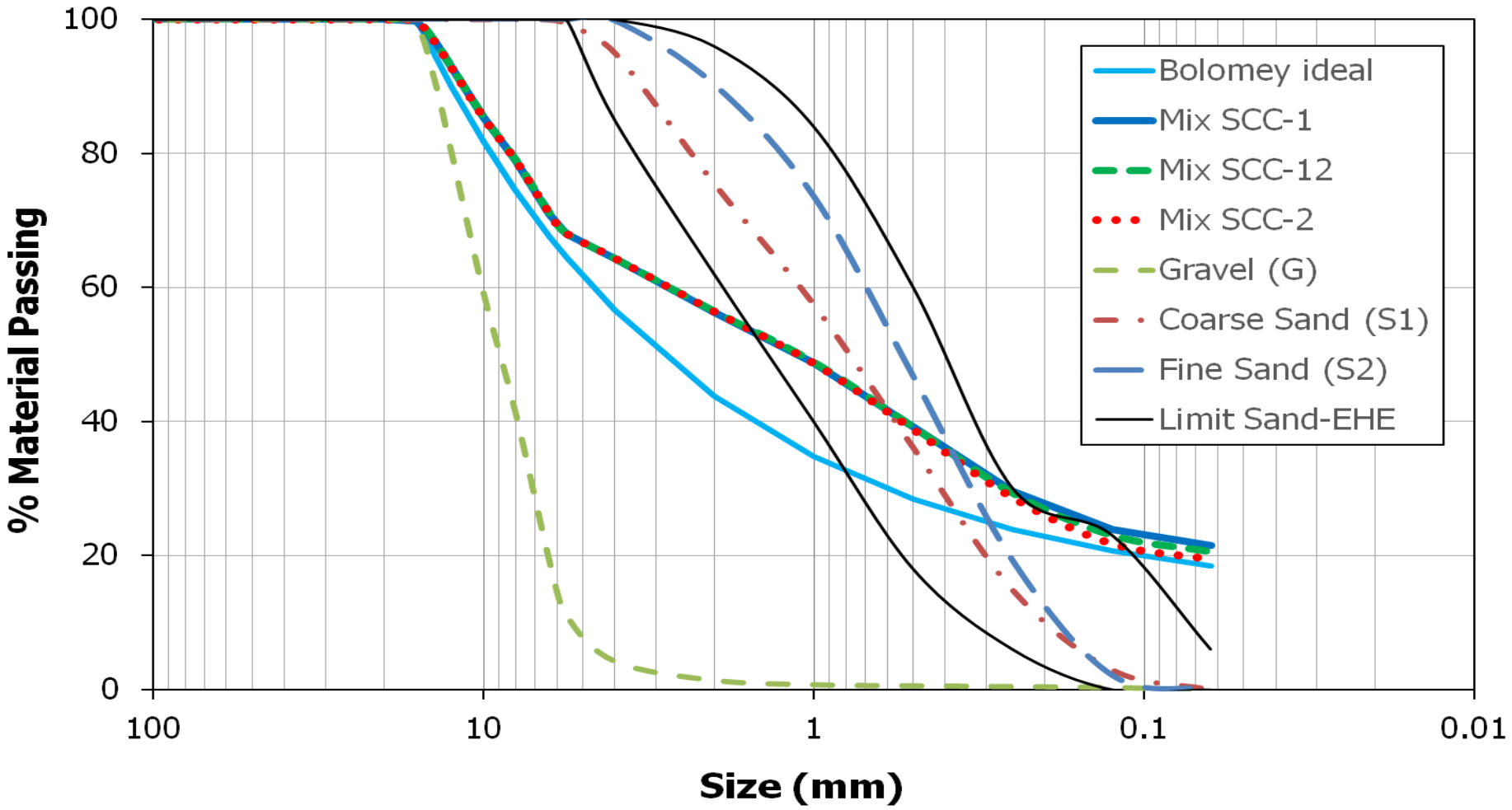


Figure 1. Particle size distribution for gravel, coarse and fine sands, mixes SCC-1, SCC-12 and SCC-2.

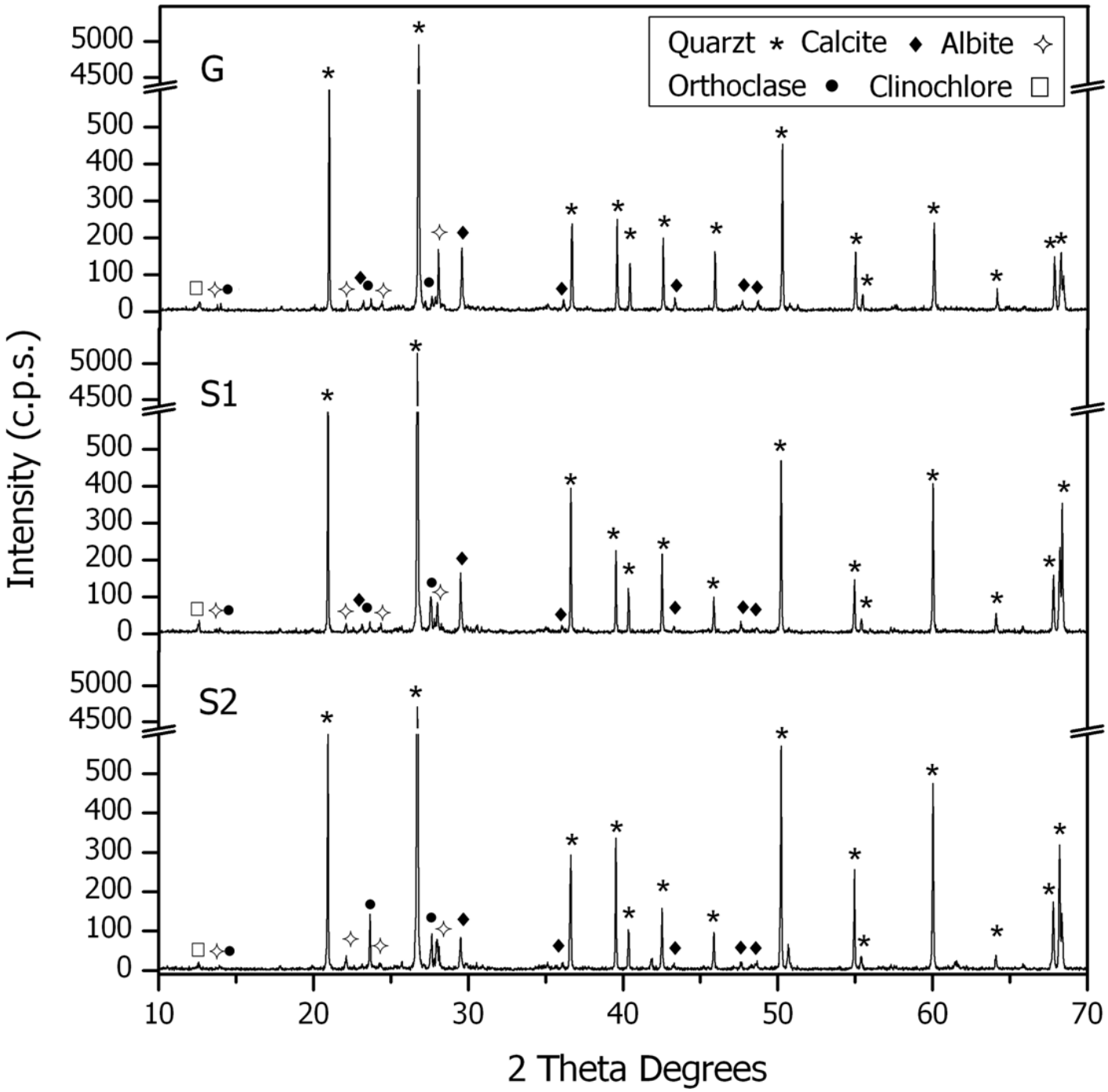


Figure 2. PXRD patterns for gravel (G), coarse (S1) and fine (S2) sands.

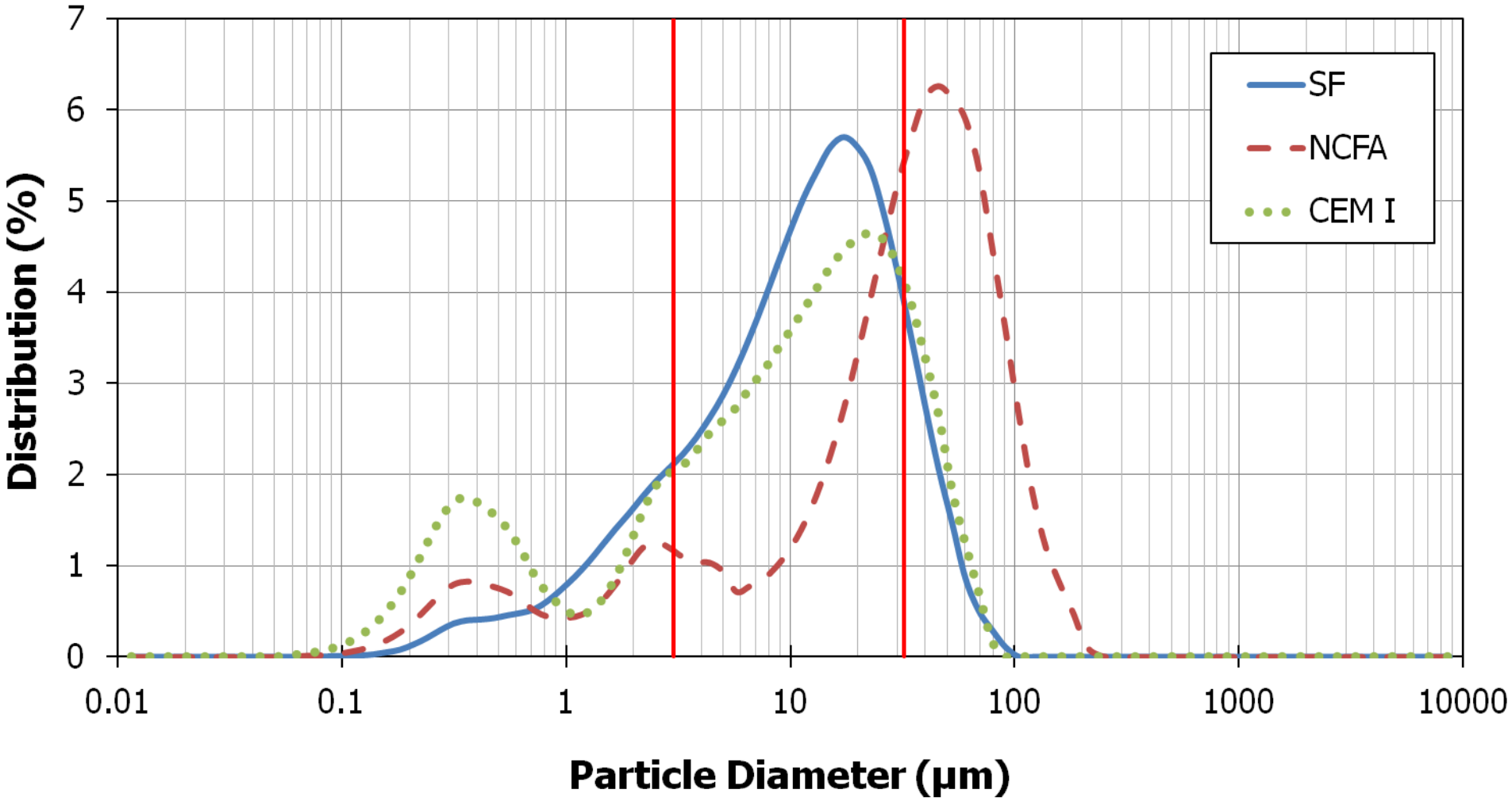


Figure 3. Grain-size distribution of SF, NCFA and CEM I by laser diffraction.

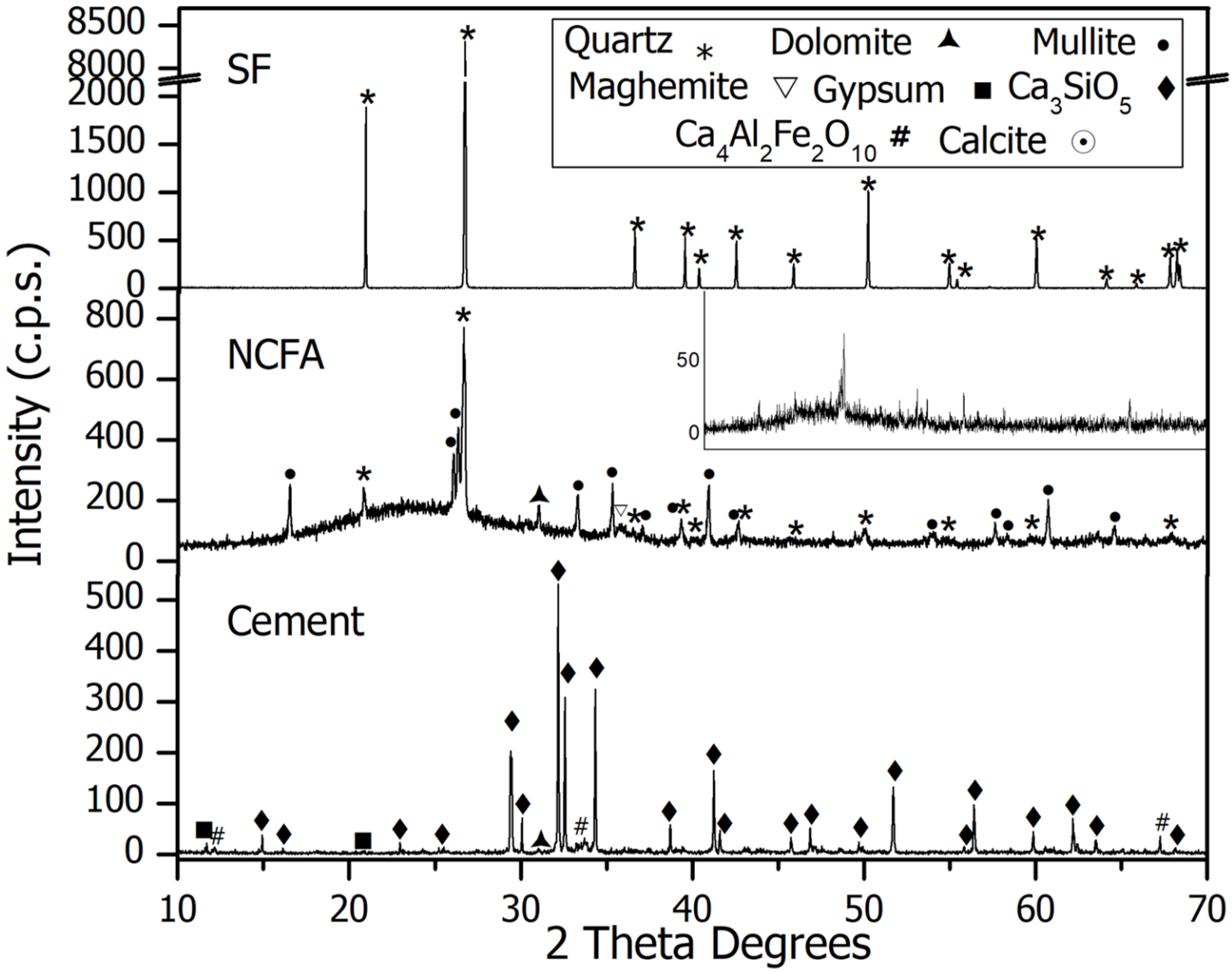


Figure 4. PXRD patterns for SF, NCFA and cement.

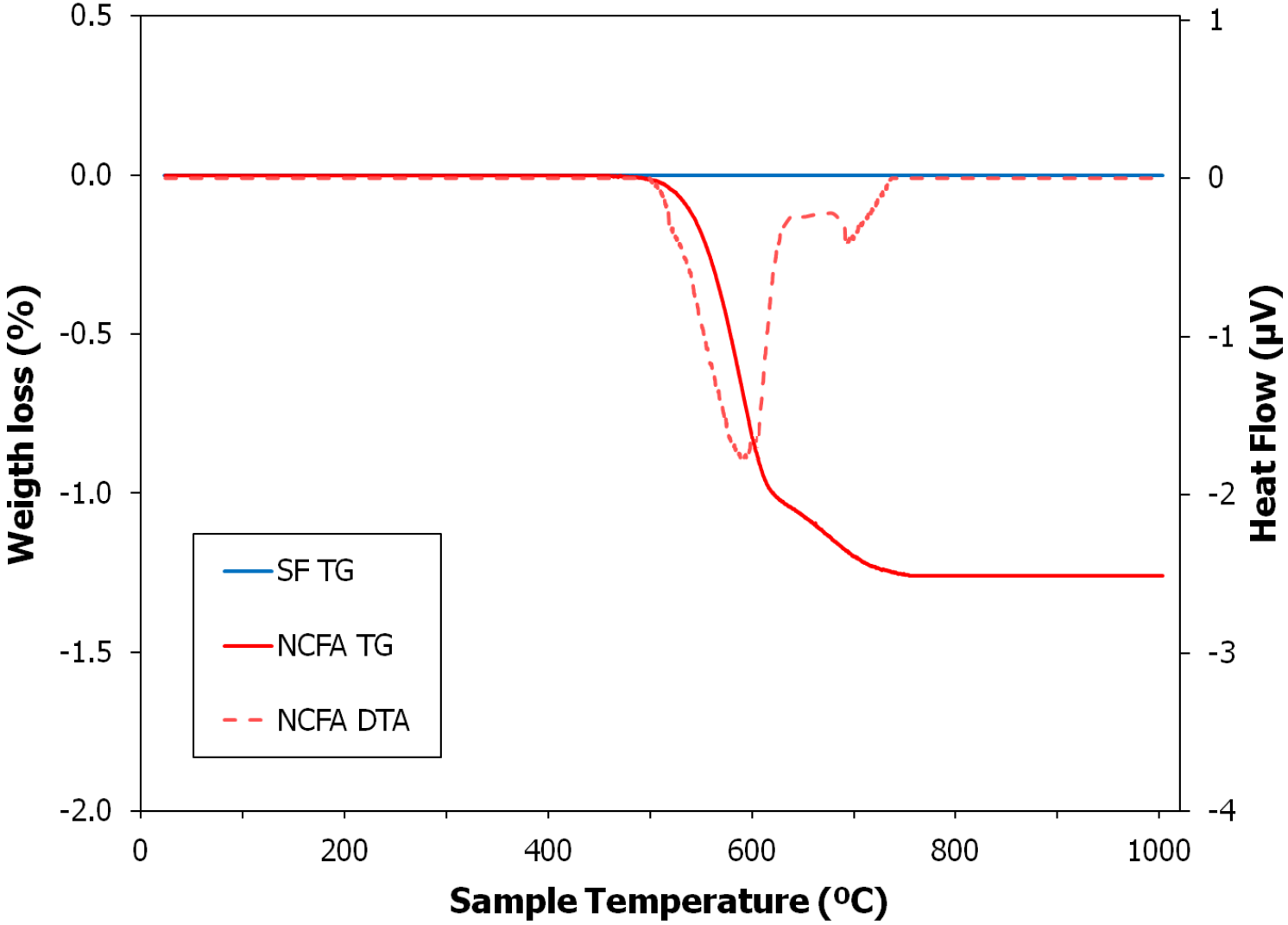


Figure 5. TG (solid lines) and DTA (dotted line) curves for the SF and NCFA fillers.

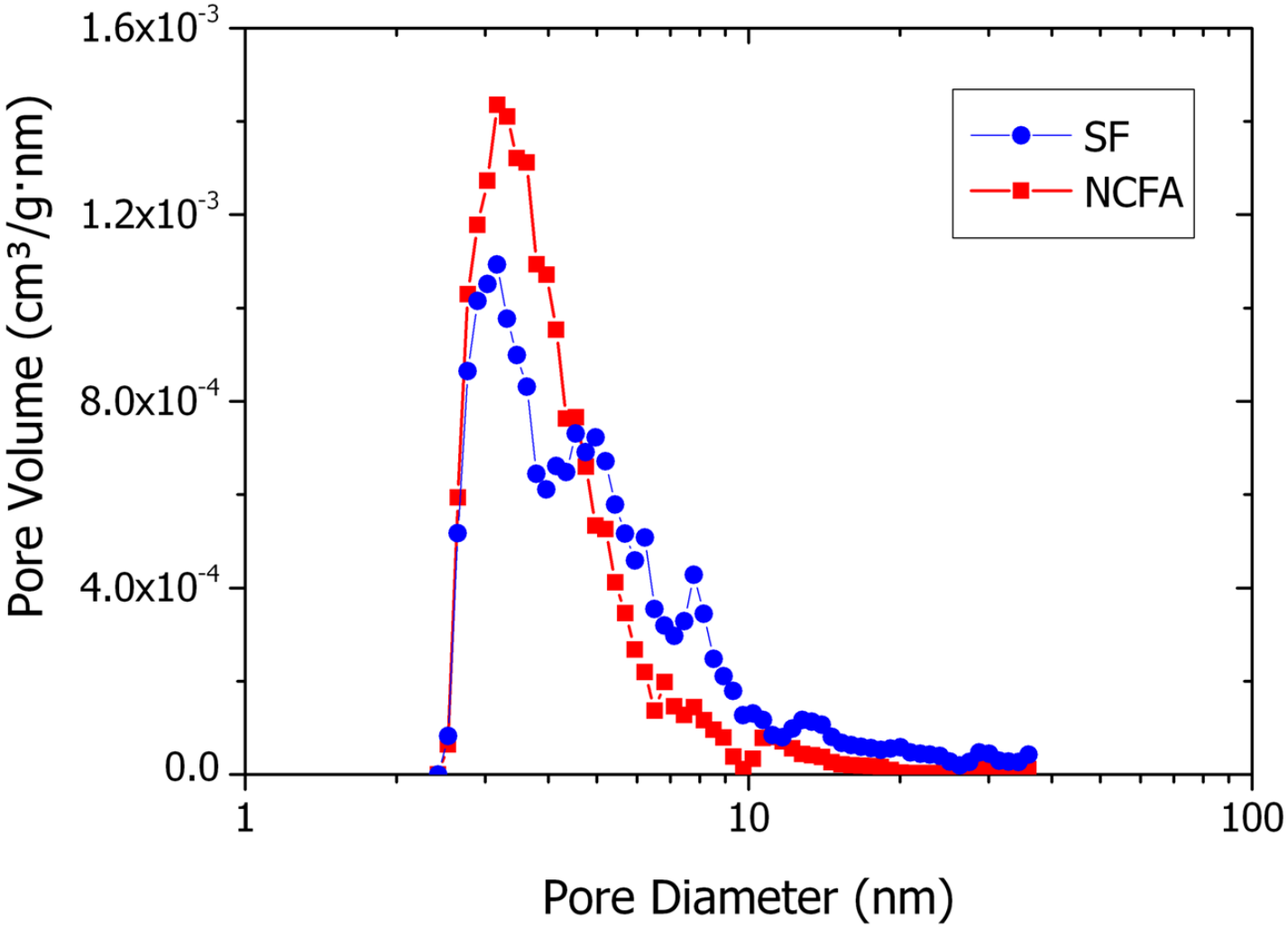


Figure 6. Pore size distribution for the SF and NCFA fillers.

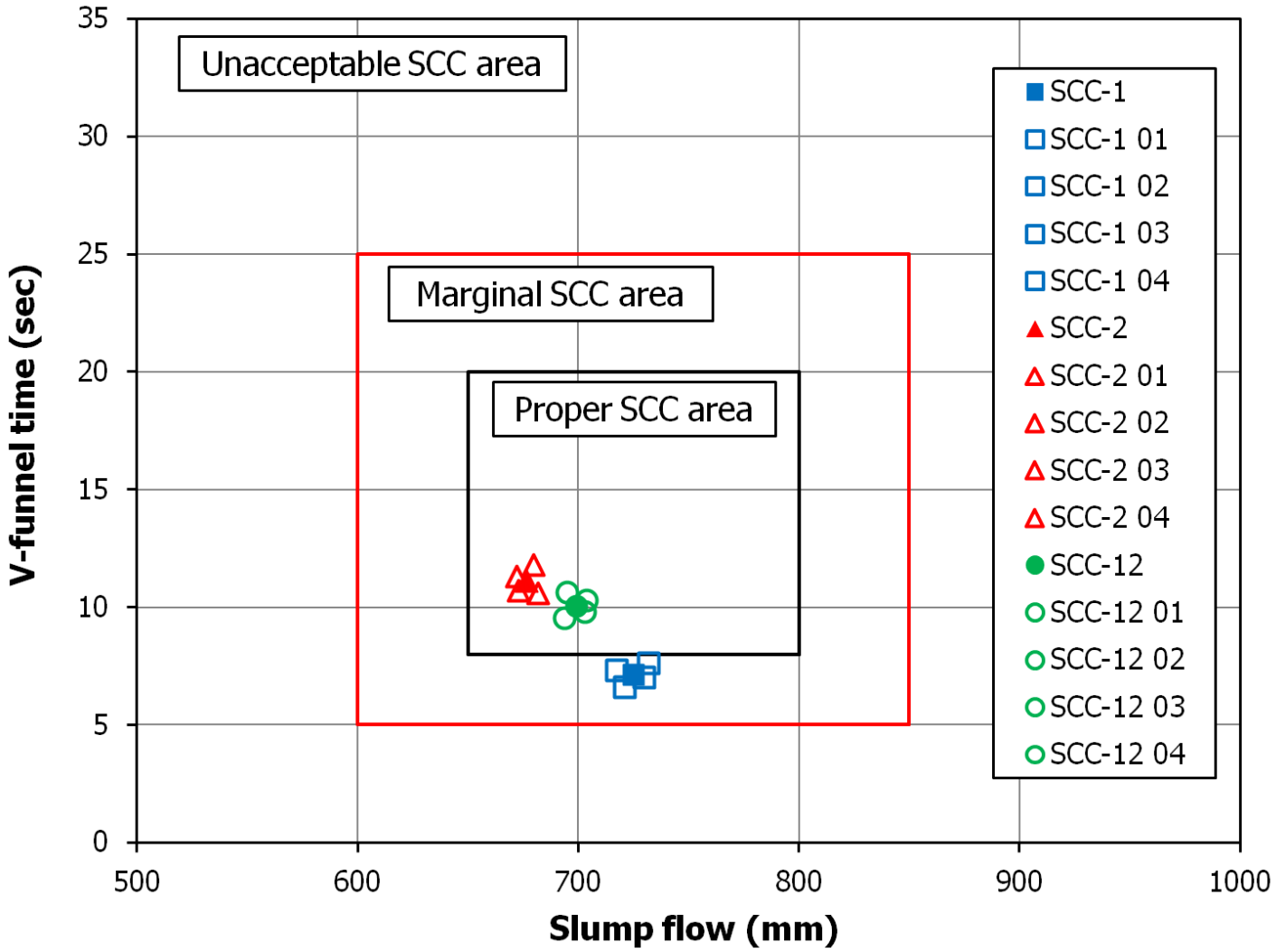


Figure 7. Workability boxes for several self-compacting mixes.

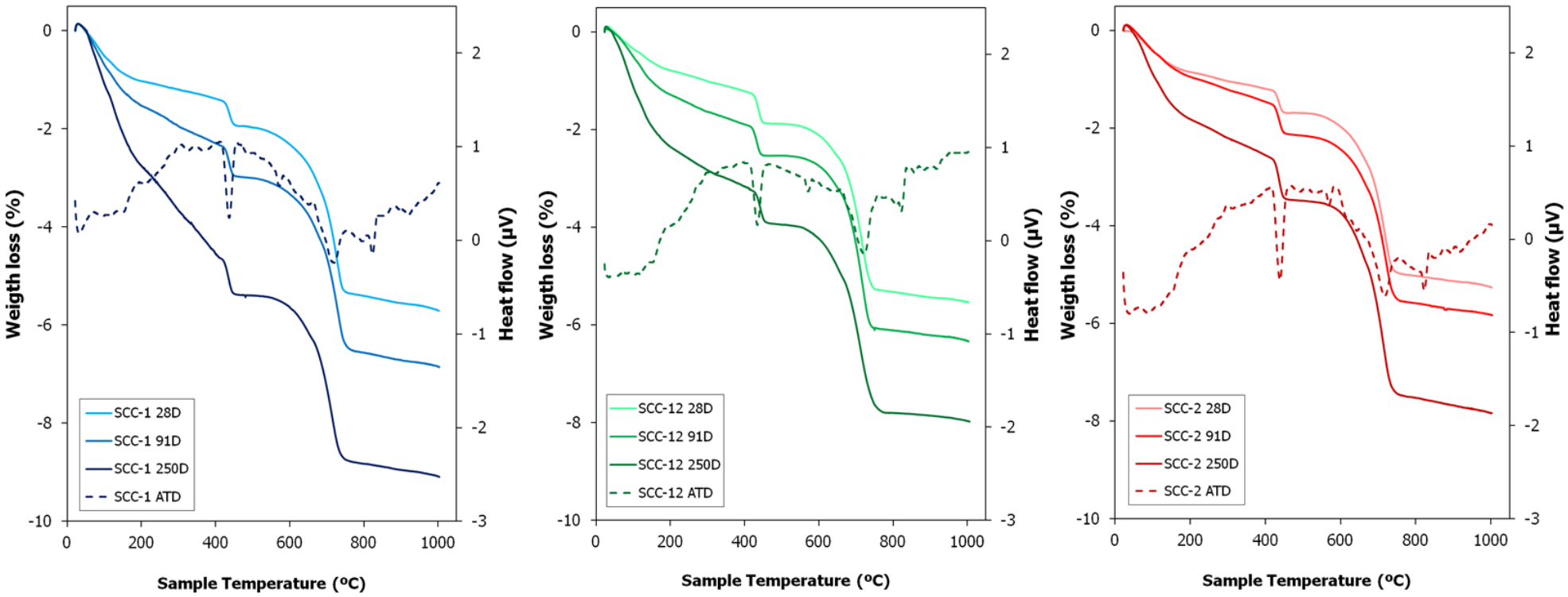


Figure 8. TGA (solid lines) and TDA (dotted lines) for several hardened SCCs.

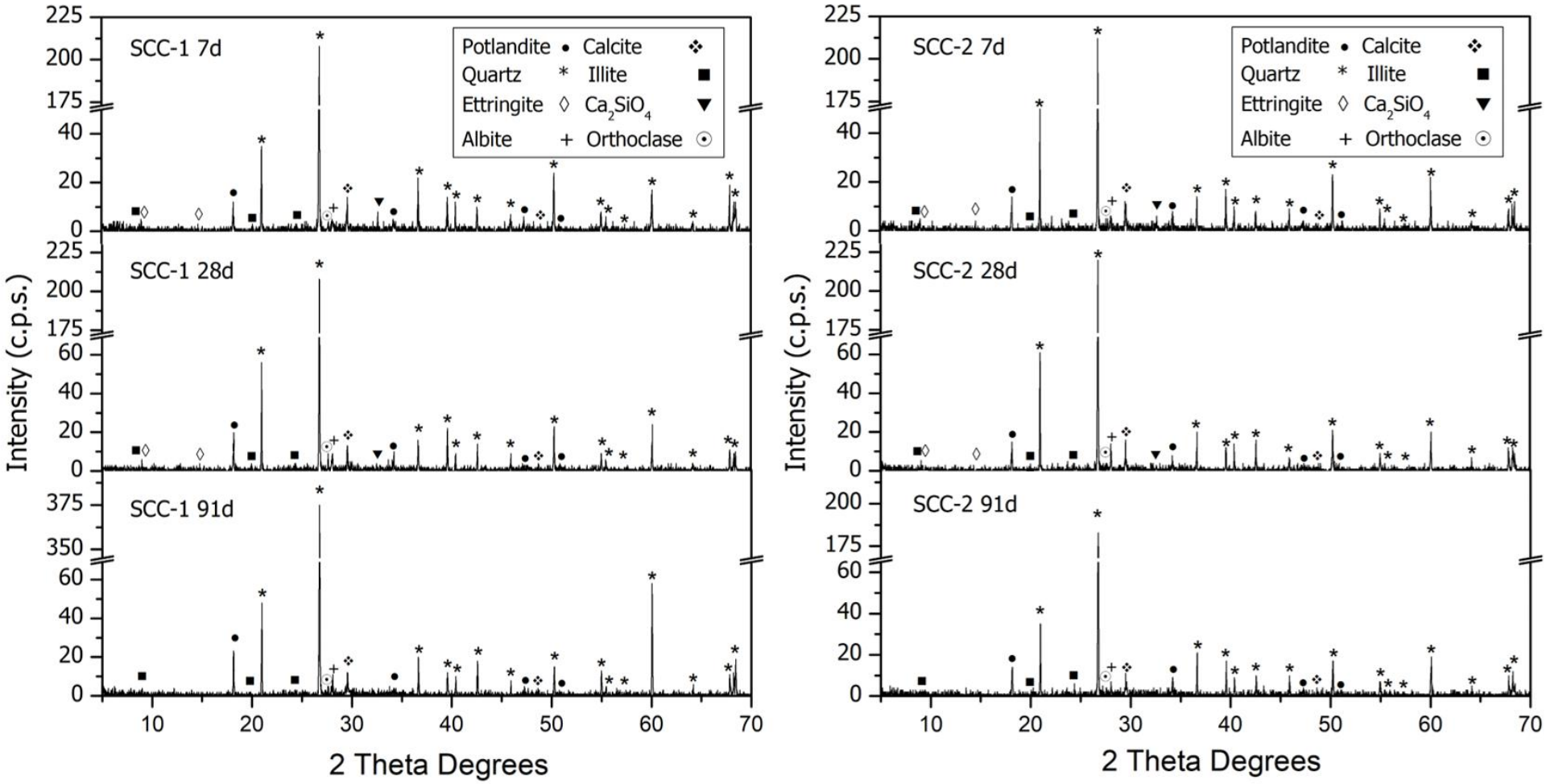


Figure 9. PXRD patterns for hardened SCC-1 and SCC-2 in the short term.

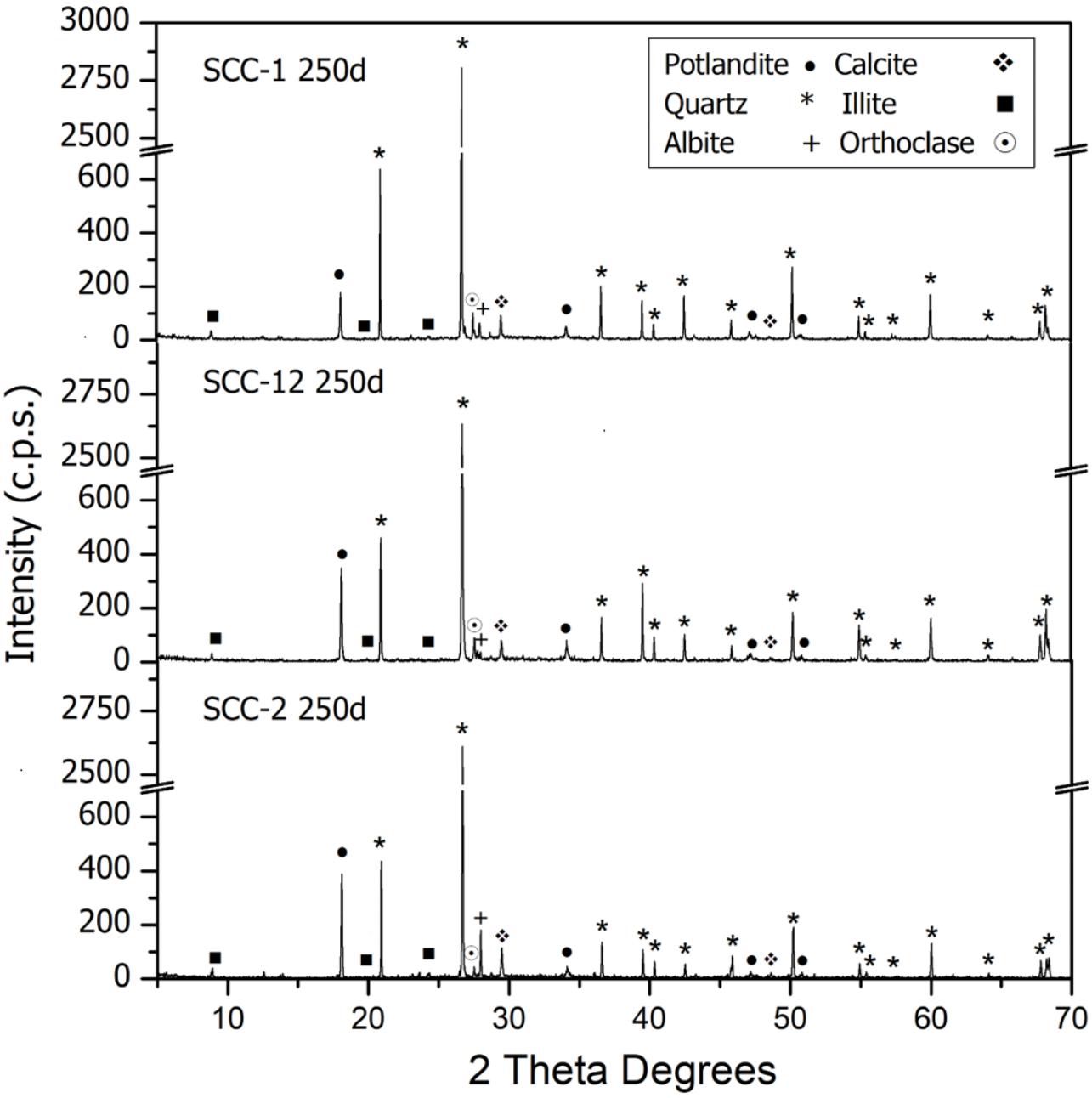


Figure 10. PXRD patterns for hardened SCC-1, SCC-12 and SCC-2 at 250 days.

.

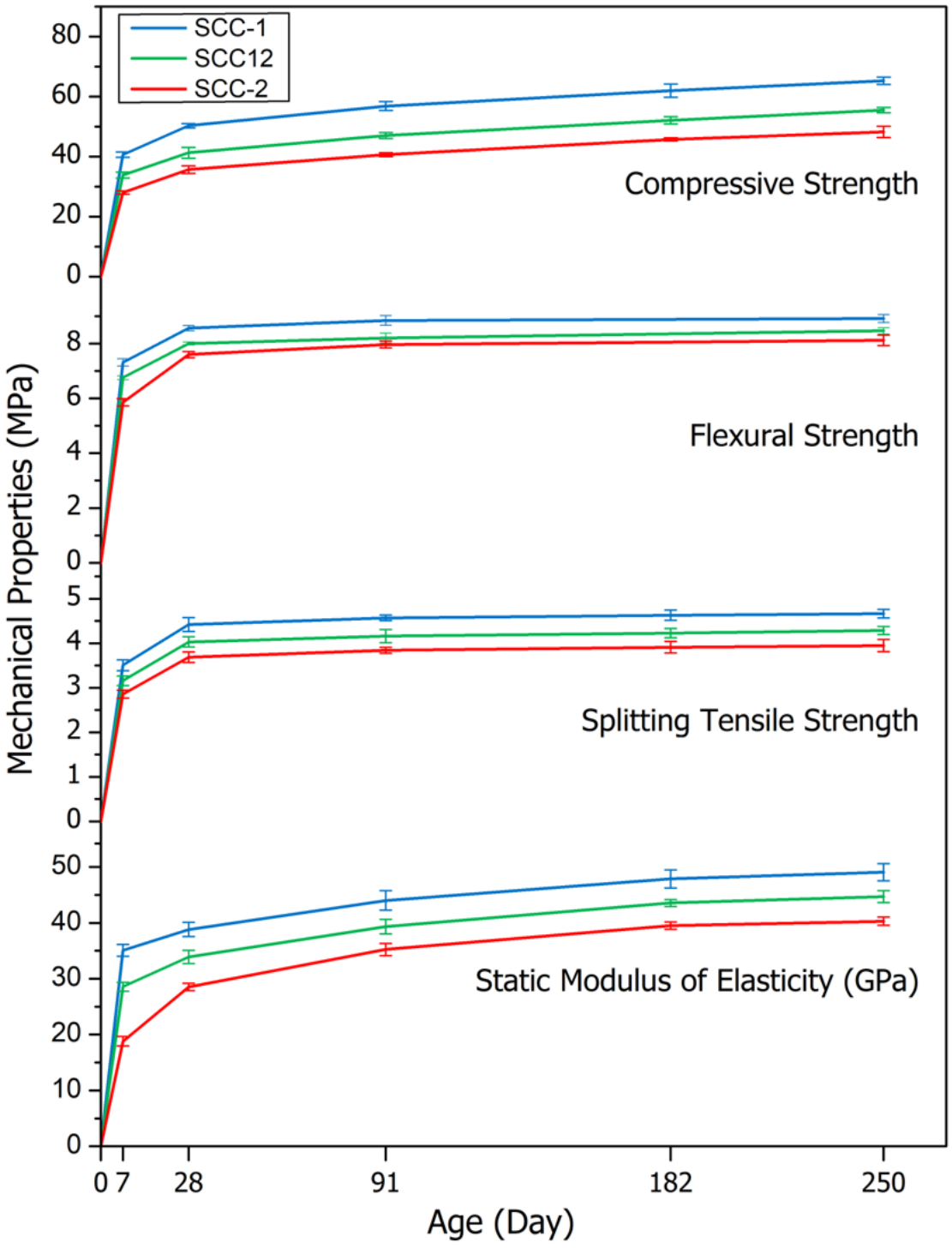


Figure 11. Mechanical properties of hardened SCCs.

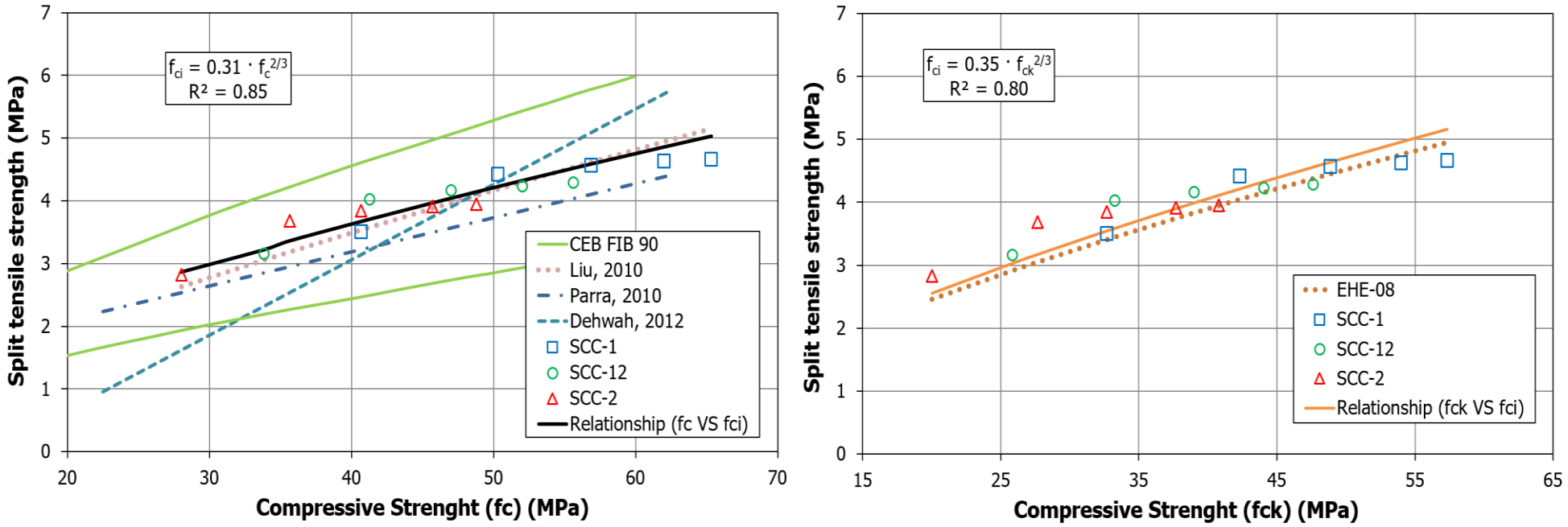


Figure 12. Compressive strength (fc) *versus* splitting tensile strength (left) and compressive strength (fck) *versus* splitting tensile strength (right).

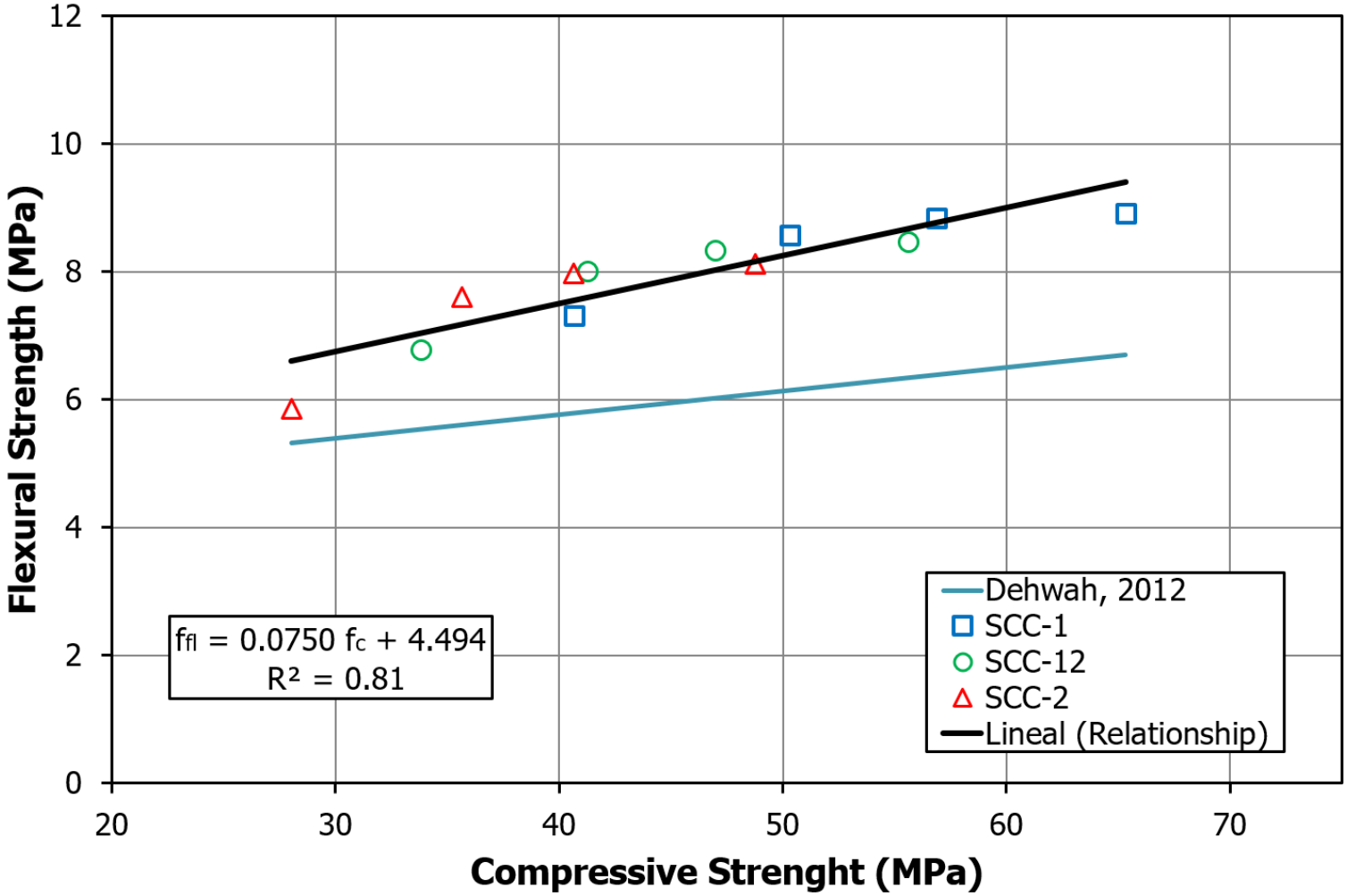


Figure 13. Compressive strength *versus* flexural strength.

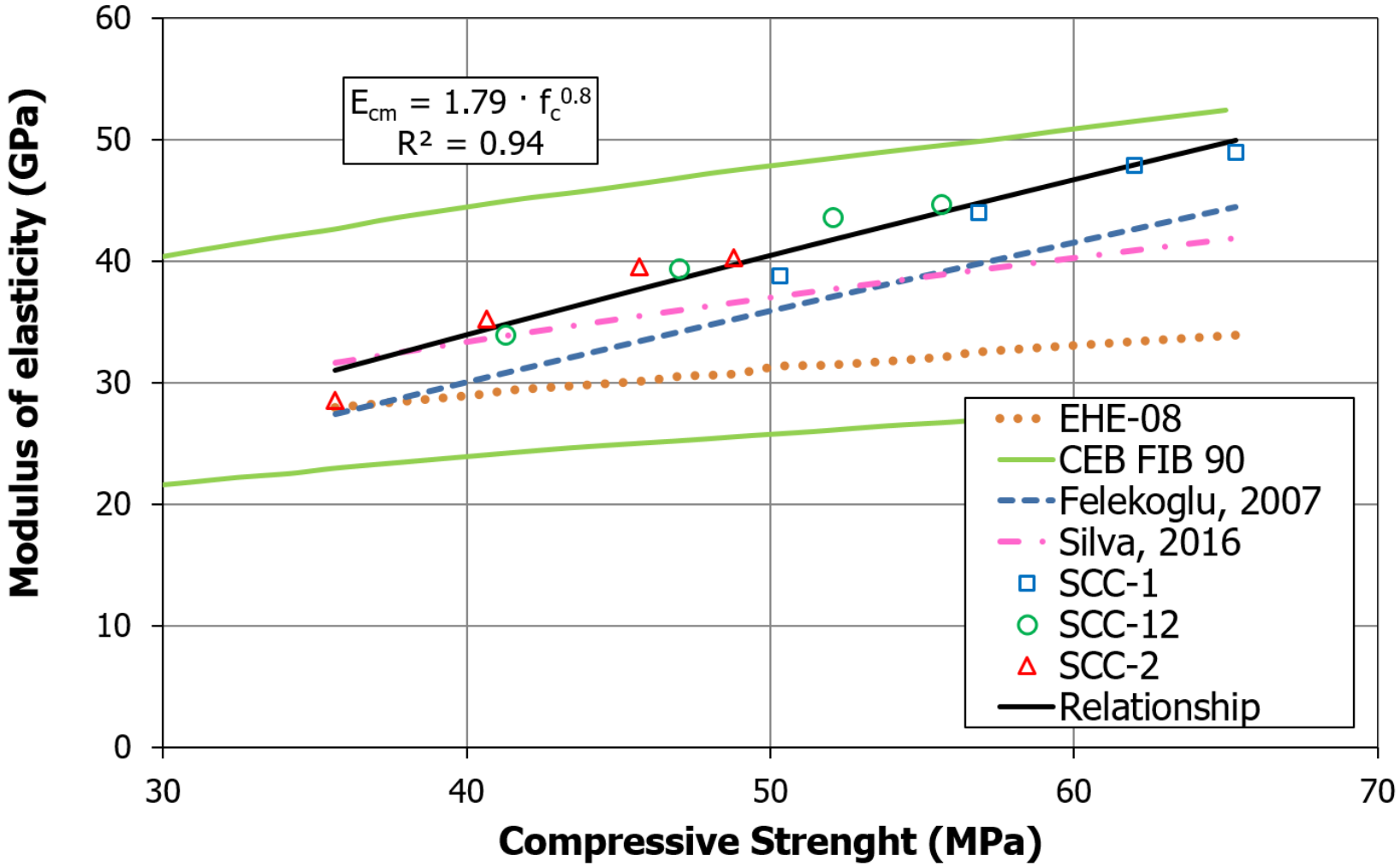


Figure 14 Compressive strength *versus* modulus of elasticity.

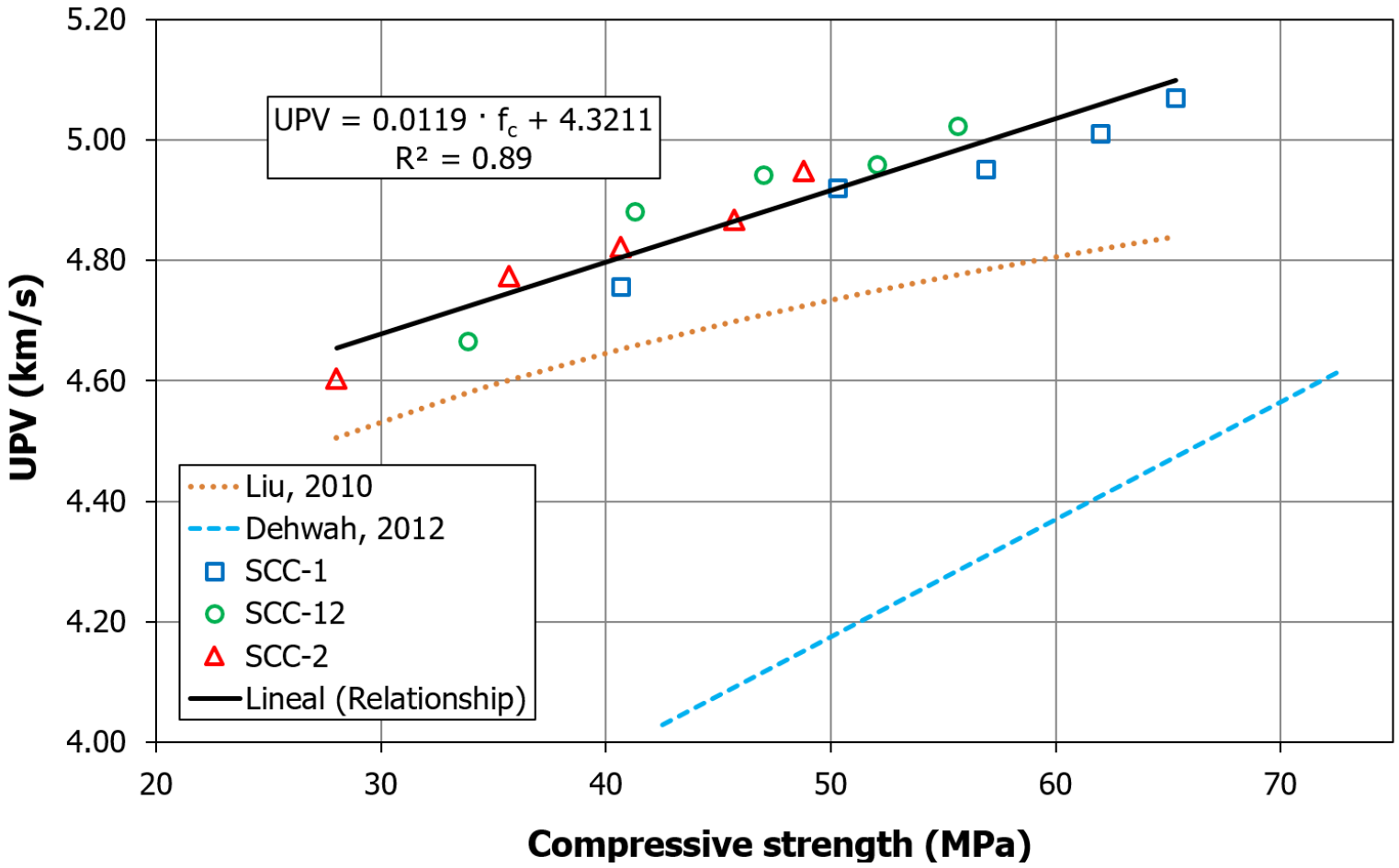


Figure 15. Compressive strength *versus* ultrasonic pulse velocity.